NOISE AND SPECTRUM ANALYSIS OF NUMERICAL DATA

June 1965 - September 1965

MATHEMATICS DEPARTMENT
UNIVERSITY OF ALABAMA
UNIVERSITY, ALABAMA

O. R. AINSWORTH

TECHNICAL REPORT
NAS8-11375 -

DCN 1-4-70-01024-01 (1F)

September, 1965

Two general approaches to the problem of power spectra estimation for stationary random processes are known. The first, originally designed for analog computers, employs a bank of handfeass filters followed by sqare law and integrating devices. This approach and the digital methods which simulate it are referred to as "direct" methods (1)*. The second, or "indirect," approach proceeds by the initial computation of the autocorrelation function, from which the power spectrum is computed by the Fourier transform (4).

This report will be concerned primarily with the direct digital approach. However, we note that Diamantides (2) describes an analog suited to the accurate, efficient evaluation of power spectra. The response of the analyzer of the analog is said to be independent of the transfer characteristic between the paired inputs and the nature of the inputs.

A direct digital method is discussed by Blackman and Tukey (1) and by Welch (3). With this method one is able to obtain estimates of the power spectrum with arbitrary resolution and accuracy at arbitrary points throughout the available frequency range. In general, the method is inferior to the direct approach, being more consumptive of machine-time. However, when the requirements for resolution and accuracy vary over the frequency range, or when it is desired to obtain estimates of the power spectrum for only a portion of the frequency range, or only in neighborhoods of a finite number of frequencies with

---

*Numbers in parentheses refer to references.

given resolution and accuracy requirements, the method is distinctly superior to the indirect digital approach.

Let x(t) denote a stationary random process. The autocorrelation function of this process is

$$(1) \qquad R(\tau) = \overline{x(t)x(t+\tau)} = \lim_{T\to\infty} \frac{1}{T}\int_0^T x(t)\,x(t+\tau)\,dt$$

which, for numerical purposes, is taken to be

$$R(\tau_j) = \frac{1}{N}\sum_i x(t_i)\,x(t_i+\tau_j)$$

the summation continuing so long as $t_i + \tau_j \le T$. Here N denotes the number of samples from the process $x(t)$, $T = t_N$, and τ_j denotes the lag time. In usual practice $\tau_j - \tau_{j-1} = t_j - t_{j-1} = \Delta t$, $\tau_k = t_k = k\,\Delta t$.

Then

$$(2) \qquad R(\tau_j) = \frac{1}{N}\sum_{i=1}^{N-j} x(t_i)\,x(t_{i+j})$$

or

$$(3) \qquad R(\tau_j) = \frac{1}{N-j}\sum_{i=1}^{N-j} x(t_i)\,x(t_{i+j})$$

The errors involved in finite time-averaging and the use of Riemann integration form the subject matter of an extensive body of literature and will not be discussed here. It can be seen from this expression that the number of arithmetic operations, multiplications in particular, required for the computation of R(t) for long records will require an excessive amount of machine-time. Thus, alternate methods for this computation have been investigated. Two of these involve the use of clipped

functions. The expressions

$$\tilde{R}(\tau_j) = \frac{1}{N-j} \sum_{i=1}^{N-j} \operatorname{sgn} x(t_i)\, x(t_{i+j}) \tag{4}$$

and

$$\hat{R}(\tau_j) = \frac{1}{N-j} \sum_{i=1}^{N-j} \operatorname{sgn} x(t_i) \operatorname{sgn} x(t_{i+j}) \tag{5}$$

are called the "half-clipped autocorrelator" or "half-polarity coincidence correlator" and the "completely-clipped autocorrelator" or "polarity coincidence correlator".

It has been shown that, if the process x(t) is zero-mean gaussian,

$$\overline{\tilde{R}(\tau_j)} = \sqrt{\frac{2}{\pi R_0}}\, R(\tau_j) \qquad (R_0 = R(0)) \tag{6}$$

i.e., the half-polarity coincidence correlator in, to within a multiplicative constant, an unbiased estimator of the true autocorrelation function. From this it follows that the normalized half-polarity coincidence correlator is an unbiased estimator of the normalized autocorrelation function. It has been suggested that, if x(t) is nongaussian, one may add uncorrelated white noise to x(t) and process the result by $\tilde{R}(\tau)$, this correlator then being denoted by $\tilde{R}'(\tau)$. The expected value of this correlator is then given to be

$$\overline{\tilde{R}'} = \frac{1}{N-j} \sqrt{\frac{2}{\pi}} \sum_{i=1}^{N-j} R \exp\left(-\frac{x^2(t_{i+j})}{2R}\right) \delta_j + \frac{1}{N-j} \sum_{i=1}^{N-j} x(t_i) \operatorname{erf}\left(\frac{x(t_{i+j})}{\sqrt{2}\, R}\right) \tag{7}$$

where

$$\delta_j = \begin{cases} 1, & m = 0 \\ 0, & m \neq 0 \end{cases}$$

$\mathcal{N}$ = rms value of added white noise.

The value of this approach in relistic situations has not been ascertained, however. We note that if the SNR ratio be sufficiently small, $\hat{R}'(\tau_j)$ is approximately an unbiased estimator for $R(\tau_j)$ when $\tau_j \neq 0$. However, the SNR of the output is also smaller, i.e., the accuracy of the scheme is reduced. For zero lag, an additional term appears, and will produce a bias of known magnitude in the power spectrum for which compensation must be made.

If x(t) be a zero-mean stationary gaussian random process, we have that, for the polarity coincidence correlator

$$(8) \qquad \overline{\hat{R}(\tau_j)} = \overline{\operatorname{sgn} x(t)\, \operatorname{sgn} x(t+\tau_j)}$$

$$= \int_{-\infty}^{+\infty}\int_{-\infty}^{+\infty} (\operatorname{sgn} p)(\operatorname{sgn} q)\, f(p,q)\, dp\, dq$$

where

$$p = x(t_i)$$

$$q = x(t_i+\tau_j)$$

$f(p,q)$ = joint probability distribution of p and q.

If the normalized autocorrelation function of the process x(t) is denoted by

$$\rho(\tau) = R(\tau)/R_0 \qquad (R_0 = R(0))$$

then

$$f(p,q) = \frac{1}{2\pi R_0^2\sqrt{1-\rho^2}} \exp\left[\frac{p^2 - 2\rho pq + q^2}{2R_0^2(1-\rho^2)}\right]$$

$$= \frac{1}{2\pi R_0^2\sqrt{1-\rho^2}} \exp\left[\frac{(q-\rho p)^2}{2R_0^2(1-\rho^2)}\right] \exp\left(-\frac{p^2}{2R_0^2}\right)$$

Hence

$$\overline{\hat{R}(\tau_j)} = \int_{-\infty}^{+\infty} df_k \, (\operatorname{sgn} f_k) \frac{1}{\sqrt{2\pi R_0^2}} e^{-f_k^2/2R_0^2} \int_{-\infty}^{+\infty} (\operatorname{sgn} g) \exp\left[\frac{-(g-\rho f_k)^2}{2R_0^2(1-\rho^2)}\right] \frac{dg}{\sqrt{2\pi R_0^2(1-\rho^2)}}$$

Now

$$(9) \quad \frac{1}{\sqrt{\pi}} \int_{-\infty}^{+\infty} (\operatorname{sgn} g) \exp\left[\frac{-(g-\rho f_k)^2}{2R_0^2(1-\rho^2)}\right] \frac{dg}{\sqrt{2R_0^2(1-\rho^2)}}$$

$$= -\frac{1}{\sqrt{\pi}} \int_{0}^{+\infty} \exp\left[\frac{-(g-\rho f_k)^2}{2R_0^2(1-\rho^2)}\right] \frac{dg}{\sqrt{2R_0^2(1-\rho^2)}} + \frac{1}{\sqrt{\pi}} \int_{0}^{+\infty} \exp\left[-\frac{(g-\rho f_k)^2}{2R_0^2(1-\rho^2)}\right] \frac{dg}{\sqrt{2R_0^2(1-\rho^2)}}$$

Letting

$$\lambda = \frac{g+\rho f_k}{\sqrt{2R_0^2(1-\rho^2)}} \quad , \quad \lambda = \frac{g-\rho f_k}{\sqrt{2R_0^2(1-\rho^2)}}$$

in the first and second integrals respectively, (9) may be written as

$$-\frac{1}{\sqrt{\pi}} \int_{\frac{\rho f_k}{\sqrt{2R_0^2(1-\rho^2)}}}^{+\infty} e^{-\lambda^2} d\lambda + \frac{1}{\sqrt{\pi}} \int_{\frac{-\rho f_k}{\sqrt{2R_0^2(1-\rho^2)}}}^{+\infty} e^{-\lambda^2} d\lambda = \frac{1}{\sqrt{\pi}} \int_{-\frac{\rho f_k}{\sqrt{2R_0^2(1-\rho^2)}}}^{\frac{\rho f_k}{\sqrt{2R_0^2(1-\rho^2)}}} e^{-\lambda^2} d\lambda$$

$$= \frac{2}{\sqrt{\pi}} \int_{0}^{\frac{\rho f_k}{\sqrt{2R_0^2(1-\rho^2)}}} e^{-\lambda^2} d\lambda = \operatorname{erf}\left(\frac{\rho f_k}{\sqrt{2R_0^2(1-\rho^2)}}\right)$$

Hence

$$\overline{\hat{R}(\tau_j)} = \frac{1}{\sqrt{2\pi R_0^2}} \int_{-\infty}^{+\infty} (\operatorname{sgn} f_k) \, e^{-f_k^2/2R_0^2} \operatorname{erf}\left(\frac{\rho f_k}{2R_0^2(1-\rho^2)}\right) df_k$$

$$= \frac{2}{\sqrt{2\pi R_0^2}} \int_{0}^{+\infty} e^{-f_k^2/2R_0^2} \operatorname{erf}\left(\frac{\rho f_k}{\sqrt{2R_0^2(1-\rho^2)}}\right) df_k$$

$$= \frac{2}{\sqrt{\pi}} \int_{0}^{+\infty} e^{-\lambda^2} \operatorname{erf}\left(\frac{\rho\lambda}{\sqrt{1-\rho^2}}\right) d\lambda \qquad \left(\lambda = \frac{\rho}{\sqrt{2}R_0}\right)$$

$$= \frac{4}{\pi} \int_{0}^{+\infty} e^{-\lambda^2} \int_{0}^{a\lambda} e^{-\mu^2} d\mu \, d\lambda \qquad \left(a = \frac{\rho}{\sqrt{1-\rho^2}}\right.$$

$$\frac{d\overline{\hat{R}(\tau_j)}}{da} = \frac{4}{\pi}\int_0^{+\infty} \lambda e^{-\lambda^2} e^{-a^2\lambda^2} d\lambda = -\frac{2}{\pi}\int_0^{+\infty} e^{-(1+a^2)\lambda^2}(-2\lambda d\lambda)$$

$$= -\frac{2}{\pi(1+a^2)} e^{-(1+a^2)\lambda^2}\Big|_0^{+\infty} = \frac{2}{\pi(1+a^2)}$$

$$\therefore \quad \hat{R}(\tau_j) = \frac{2}{\pi}\arctan a + C$$

$C = 0$ since $\overline{\hat{R}(0)} = 0$

$$\overline{\hat{R}(\tau_j)} = \frac{2}{\pi}\arctan\frac{\rho}{\sqrt{1-\rho^2}} = \frac{2}{\pi}\arcsin\rho$$

and

$$R(\tau_j) = R_0 \sin\left[\frac{\pi}{2}\overline{\hat{R}(\tau_j)}\right] \tag{10}$$

We have considered the use of clipped power spectra having the forms

$$\tilde{P}(\omega) = \int_0^{+\infty} R(\tau)\,\mathrm{sgn}\cos\omega\tau \cong \frac{1}{N}\sum_{j=1}^{N} R(\tau_j)\,\mathrm{sgn}\cos\omega\tau_j \tag{11}$$

$$\tilde{P}_1(\omega) = \int_0^{+\infty} \mathrm{sgn}\,R(\tau)\cos\omega\tau \cong \frac{1}{N}\sum_{j=1}^{N} \mathrm{sgn}\,R(\tau_j)\cos\omega\tau_j \tag{12}$$

$$\hat{P}(\omega) = \int_0^{+\infty} \mathrm{sgn}R(\tau)\,\mathrm{sgn}\cos\omega\tau\, d\tau \cong \frac{1}{N}\sum_{j=1}^{N} \mathrm{sgn}R(\tau_j)\,\mathrm{sgn}\cos\omega\tau_j \tag{13}$$

as estimators of the true power spectrum

$$P(\omega) = \frac{2}{\pi}\int_0^{\infty} R(\tau)\cos\omega\tau\, d\tau \cong \frac{2}{\pi N}\sum_{j=1}^{N} R(\tau_j)\cos\omega\tau_j \tag{14}$$

The expectation of the first of these estimators is given by an integral of the form

$$\overline{\tilde{P}(\omega)} = \int_{-\infty}^{+\infty} \int_{-\infty}^{+\infty} p \operatorname{sgn} q \; h(p,q)\, dp\, dq \tag{15}$$

where $p = R(\tau)$, $q = \cos \omega\tau$, and $h(p,q)$ is the joint probability distribution of p and q. However, since nothing is known concerning this distribution, the evaluation of the expectation integral cannot be accomplished directly. Similar considerations apply to the remaining proposed estimators. The corresponding expectation integrals have thus far proven intractible.

Experimental results to be discussed presently indicate that these estimators can be of some utility. We have observed that if $P(\omega)$ has a maximum at $\omega = \omega_0$ then so also do $\tilde{P}(\omega)$, $\tilde{P}_1(\omega)$ and $\hat{P}(\omega)$.

Consider the function sgn $\cos \omega\tau$. This (even) function has the Fourier series representation

$$\operatorname{sgn} \cos \omega\tau = \sum_n a_n \cos n\omega\tau$$

where

$$a_n = \frac{\omega}{\pi} \int_0^{\pi/2\omega} \cos n\omega\tau \, d\tau - \frac{\omega}{\pi} \int_{\pi/2\omega}^{\pi/\omega} \cos n\omega\tau \, d\tau$$

$$= \frac{1}{n\pi} \sin n\omega\tau \Big|_0^{\pi/2\omega} - \frac{1}{n\pi} \sin n\omega\tau \Big|_{\pi/2\omega}^{\pi/\omega} = \frac{2}{n\pi} \sin \frac{n\pi}{2}$$

$$= \begin{cases} 0, & n \text{ even} \\ \frac{2}{(2n+1)\pi}(-)^n, & n \text{ odd} \end{cases}$$

$$\therefore \quad \operatorname{sgn} \cos\omega\tau = \frac{2}{\pi} \sum_{k=0}^{\infty} \frac{(-)^k}{2k+1} \cos(2k+1)\omega\tau$$

and

$$\tilde{P}(\omega) = \int_0^{+\infty} R(\tau) \operatorname{sgn}\cos\omega\tau \, d\tau = \frac{2}{\pi} \sum_{k=0}^{\infty} \frac{(-)^k}{2k+1} \int_0^{+\infty} R(\tau) \cos(2k+1)\omega\tau \, d\tau$$

or

$$(16) \quad \tilde{P}(\omega) = \sum_{k=0}^{\infty} \frac{(-)^k}{2k+1} P[(2k+1)\omega]$$

$$= P(\omega) - \tfrac{1}{3} P(3\omega) + \tfrac{1}{5} P(5\omega) - \cdots$$

Suppose now that ω_0 is a peak frequency and that $P(\omega)$ is essentially flat for $\omega \geq 3\omega_0$, i.e., the noise at all higher frequencies is white. Then we may write

$$\tilde{P}(\omega_0) \cong P(\omega_0) + P(3\omega_0)\left[\left(1 - \tfrac{1}{3} + \tfrac{1}{5} - \cdots\right) - 1\right]$$

$$\cong P(\omega_0) + P(3\omega_0)\left[\log 2 - 1\right]$$

$$(17) \quad \tilde{P}(\omega_0) \cong P(\omega_0) + .307\, P(3\omega_0)$$

If $\omega_1 \geq 3\omega_0$ then we have that $P(\omega_1), P(3\omega_1), \ldots$ are all approximately equal. Hence

$$\tilde{P}(\omega_1) \cong P(\omega_1)\left[1 - \tfrac{1}{3} + \tfrac{1}{5} - \cdots\right] = P(\omega_1)\log 2$$

or

$$P(\omega_1) \cong \frac{1}{\log 2} \tilde{P}(\omega_1)$$

Since $P(\omega_1) \cong P(3\omega_0)$,

$$\tilde{P}(\omega_0) \cong P(\omega_0) + \frac{.307}{\log 2} \tilde{P}(\omega_1)$$

or

$$(18) \quad P(\omega_0) = \left[\tilde{P}(\omega_0) - \frac{.307}{\log 2} \tilde{P}(\omega_1)\right]$$

The assumptions made in the derivation of this expression were

(i) ω_0 is the largest data frequency

(ii) $P(\omega)$ is nearly constant for $\omega \geq 3\omega_0$.

Now $\tilde{P}(\omega_0) - \tilde{P}(\omega_1) = P(\omega_0) + .307\,P(\omega_1) - P(\omega_1)\log 2$

$= P(\omega_0) + \log 2\, P(\omega_1) - P(\omega_1) - P(\omega_1)\log 2$

(19) $\tilde{P}(\omega_0) - P(\omega_1) = P(\omega_0) - P(\omega_1)$

Thus, under the assumptions $\tilde{P}(\omega)$ and $P(\omega)$ decrease together for $\omega > \omega_0$. If the assumption (i) is changed to read "ω_0 is the only data frequency", then we may state that $P(\omega_0)$ and $\tilde{P}(\omega_0)$ have a peak at $\omega = \omega_0$.

For special, but not unrealistic, assumptions, the relation (16), which gives the cosine-clipped power spectrum $\tilde{P}(\omega)$ in terms of a series in the power spectrum $P(\omega)$, can be reversed to express the power spectrum in terms of a series in $\tilde{P}(\omega)$. As an example, consider the following:

$$\tilde{P}(\omega_0) = P(\omega_0) - \tfrac{1}{3}P(3\omega_0) + \tfrac{1}{5}P(5\omega_0) - \tfrac{1}{7}P(7\omega_0) + \tfrac{1}{9}P(9\omega_0) - \cdots$$

$$\tfrac{1}{3}\tilde{P}(\omega_0) = \qquad + \tfrac{1}{3}P(3\omega_0) \qquad\qquad - \tfrac{1}{9}P(9\omega_0) + \cdots$$

$$-\tfrac{1}{5}\tilde{P}(\omega_0) = \qquad\qquad -\tfrac{1}{5}P(5\omega_0) + \cdots$$

$$\tfrac{1}{7}\tilde{P}(\omega_0) = \qquad\qquad\qquad + \tfrac{1}{7}P(7\omega_0) - \cdots$$

where ω_0 is some data frequency of interest. Now if it is assumed that $P(\omega)$ is essentially zero for $\omega > K$ where $9\omega_0 \leq K < 11\omega_0$ then we have, by adding the above, that

(20) $$P(\omega_0) = \tilde{P}(\omega_0) + \tfrac{1}{3}\tilde{P}(3\omega_0) - \tfrac{1}{5}\tilde{P}(5\omega_0) + \tfrac{1}{7}P(7\omega_0)$$

It is obvious that this type of relation may be obtained for different assumptions and approximations. However, in many cases, the assumptions used in deriving (20) will be satisfied when ω_o is fairly "large".

The process of inverting (16) leads to the series

$$\begin{aligned} P(\omega) = \tilde{P}(\omega) &+ \tfrac{1}{3}\tilde{P}(3\omega) - \tfrac{1}{5}\tilde{P}(5\omega) + \tfrac{1}{7}\tilde{P}(7\omega) + \tfrac{1}{11}\tilde{P}(11\omega) - \tfrac{1}{13}\tilde{P}(13\omega) \\ &- \tfrac{1}{15}\tilde{P}(15\omega) - \tfrac{1}{17}\tilde{P}(17\omega) + \tfrac{1}{19}\tilde{P}(19\omega) + \tfrac{1}{21}\tilde{P}(21\omega) \\ &+ \tfrac{1}{23}\tilde{P}(23\omega) - \tfrac{1}{29}\tilde{P}(29\omega) + \tfrac{1}{31}\tilde{P}(31\omega) + \tfrac{1}{33}\tilde{P}(33\omega) \\ &- \tfrac{1}{35}\tilde{P}(35\omega) - \tfrac{1}{37}\tilde{P}(37\omega) - \tfrac{1}{41}\tilde{P}(41\omega) + \tfrac{1}{43}\tilde{P}(41\omega) \\ &+ \tfrac{1}{47}\tilde{P}(47\omega) - \tfrac{1}{51}\tilde{P}(51\omega) - \tfrac{1}{53}\tilde{P}(53\omega) - \tfrac{1}{56}\tilde{P}(55\omega) \\ &+ \tfrac{1}{57}\tilde{P}(57\omega) + \tfrac{1}{59}\tilde{P}(59\omega) - \tfrac{1}{61}\tilde{P}(61\omega) \cdots \end{aligned}$$

This can be written

$$P(\omega) = \sum_{i=1}^{\infty} \frac{(-)^{f(k_i)}}{k_i} \tilde{P}(k_i\omega) \tag{21}$$

where the k_i are the square-free odd integers. (An integer is said to be square-free if, in representing it as a product of prime factors, no factor is repeated.) An expression for $f(k_i)$ does not seem to be obvious. However, the problem is interesting and will be considered further. If, and when, this expression is found, it will be communicated to the technical representative.

The experimental results indicate that even when the assumptions made in deriving these results are violated, the clipped function technique can be used to detect data frequencies with a fairly high degree of reliability. Table 1.1 lists the predominant frequencies in a Saturn static firing

vibration record as compiled by NSFC's RAVAN (Random Vibration Analysis) program. The measurement number of this record is E106-11, the time interval considered being 15.0 to 16.0 seconds. These frequencies are numbered according to amplitude.

Table 1.2 lists the "predominant" frequencies for the same record by this program, modified to give a half-polarity correlator. The amplitudes are obviously garbled. The missing frequencies are apparently 2, 3, 6, 8, 10, 12, 15, 18, 20. A careful examination of the power spectrum shows that only the last three were not detected. The remaining frequencies were subjected to slight shifts, and the corresponding frequencies are numbered in parentheses. We note that the value of $\Delta\omega$ used in computing these frequencies was 5.0, and that the shifts to which these data frequencies were subjected is one or two times this value. We are thus led to suspect that this error is due to some such source as truncation, and does not reflect on the accuracy of the clipping technique in frequency determination. Three apparently spurious frequencies are indicated. The first, 705.110 001 is found to correspond to a doubling in magnitude between 700.110 001 and this frequency. The second, 935.145 889, corresponds to a weak data frequency or local maximum in the standard case of 930.145. Again, the shift is of magnitude $\Delta\omega$. The third frequency, 555.086 594, appears to be genuinely spurious, and is possibly the result of the data frequency 545.085 037 being detected twice. If so, the shift is of magnitude $2\Delta\omega$.

Table 1.3 lists the "predominant" frequencies compiled by RAVAN modified to give a cosine-clipped power spectrum. The missing frequencies here are 345.053 829, 275.042 908, and 95.014 823, which are numbered 11, 19, and 20, respectively, in the standard case. The first two of these were detected, but were not listed due to the garbling of amplitudes. The last was shifted to 90.014 (a shift of magnitude $\Delta\omega$) and was not listed for the same reason. The three additional data frequencies in this list were found to correspond to minor peaks in the standard power spectrum, and are not at all spurious.

Table 1.4 lists the "predominant" frequencies compiled by RAVAN modified to compute a cosine-clipped power spectral density function from a half-polarity correlator. The missing frequencies are here apparently 345.053 829, 1105.172 409, 95.014 823, and 275.042 908, these being numbered 11, 14, 19, and 20, respectively, in the standard case. The first and last of these appear as peaks in the power spectrum computed here, but were not listed due to the garbling of amplitudes. The two remaining frequencies were shifted to 1000.157 and 90.014 respectively, were detected, and were not listed for the same reason. Of the apparently spurious frequencies, 735.114 677 corresponds to a weak data frequency, and was also detected when a cosine-clipped power spectrum was computed from a standard autocorrelation function. The frequency 555.086 594 appeared when the standard power spectrum was computed from

the half-polarity correlator and is discussed above. An examination of the power spectrum computed in the standard case indicates that the frequency 1000.156 029 may result from detecting the frequency 990.154 472 twice. The last apparently spurious frequency, 705.110 001, was listed in Table 1.2 and discussed above.

Considering the nature of the assumptions made in deriving (18) and (19), the implications of (21), and the exceedingly good results obtained here, it is apparent that the use of the half-clipped power spectrum can be of great advantage when it is of interest to determine data frequencies, particular when the energy in frequencies beyond a certain value is nearly zero. The equations (20) and (21) suggest that the value of the power spectrum for a certain value of can be recovered from the cosine-clipped power spectrum.

Table 1.5 lists the "predominant" frequencies as compiled by RAVAN modified to give a polarity coincidence correlator. The missing frequencies are 990.154 472, 1105.172 409, and 275.042 908, these being numbered 8, 14, and 20 in the standard case. The last was detected, but was not listed due to the garbling of amplitudes. The first was shifted to 995.155 (the shift being of magnitude $\Delta\omega$) was detected, and was not listed for the same reason. The remaining missing frequency was apparently not detected. The two additional frequencies were encountered in the preceeding cases and are discussed above.

Table 1.6 lists the "predominant" frequencies as compiled by RAVAN modified to give a completely clipped power spectral

density function. The missing frequencies are 480.074 894, 345.053 829, 1105.172 409, 1045.163 055, and 275.042 908, which are numbered 9, 11, 14, 16, and 20, respectively, in the standard case. The first, second, and fourth of these frequencies were detected, but were not listed due to the garbling of amplitudes. The last was shifted to 270.042 (the shift being of magnitude $\Delta\omega$), and was not listed due to the garbling of amplitudes. Of the remaining frequencies in this list, namely 790.123 260, 1580.246 521, 215.033 546, 2030.316 742, and 625.097 519, the first four correspond to minor peaks of the power spectrum computed in the standard case. The fifth appears to be entirely spurious.

Table 1.7 lists the "predominant" frequencies as compiled by RAVAN modified to compute a completely clipped power spectral density function from a polarity coincidence correlator. The missing frequencies here are

6	500.078 014
7	300.046 810
8	990.154 472
10	720.112 343
12	545.085 037
14	1105.172 409
16	1045.163 055
20	275.042 908

where the integers denote the numbering of these frequencies. Of these, only the last was not detected. The first, fourth,

fifth and sixth frequencies were subjected to shifts of magnitude $\Delta\omega$, were detected, but were not listed due to the garbling of amplitudes. The remaining frequencies were detected without shifting, and were not listed for the same reason.

Table 2.1 lists the predominant frequencies as compiled by the unmodified RAVAN program, and will be subsequently referred to as the "standard case". The power spectra and RMS amplitudes for this set of data are given in decibel units.

Table 2.2 lists the predominant frequencies compiled by RAVAN modified to compute the half-polarity autocorrelator. The missing frequencies here are

16	2604.597 168
17	2574.601 807

the integers referring to the numbering of these frequencies in the standard case. The first of these was detected, but was not listed due to the garbling of amplitudes. The second, which is a relatively weak frequency, does not seem to have been detected. The two additional frequencies listed are 614.904 900 and 454.929 642. The first reflects a weak frequency appearing in the standard case which was not listed there because of its low energy content. The second frequency may result from detecting the frequency 444.931 190 twice, or may be genuinely spurious.

Table 2.3 lists the "predominant" frequencies compiled by RAVAN modified to compute a cosine-clipped power spectrum from the standard autocorrelator. The missing frequencies here are

16	2604.597 168
19	2539.607 239.

Both of these were detected, but were not listed due to the garbling of amplitudes. The second of these frequencies was detected as 2544.606, but was not listed due to the garbling of amplitudes. The two additional frequencies listed in this table are 454.929 642 and 3159.511 353. The first has been encountered and discussed above. The last seems to be genuinely spurious. We remark that this is a case in which the cosine-clipped power spectrum is as effective in frequency determination as is the conventional spectrum.

Table 2.4 lists the "predomi[illegible] frequencies as compiled by RAVAN modified to compute cosi[illegible]-clipped power spectrum from a half-polarity autocorrelator. The missing frequencies in this list are

16	2604.597 168
17	2574.601 807
18	939.854 645,

the integers referring to the numbering of these frequencies in the standard case. All three of these frequencies were detected, but were not listed due to the garbling of amplitudes. The apparently spurious frequencies are

454.929 642
3159.511 353
2659.588 684.

The first two of these have been encountered previously and are discussed above. The third corresponds to a weak frequency detected in the standard case but not listed there because of its low energy content.

Table 2.5 listed the predominant frequencies compiled by RAVAN modified to compute a polarity coincidence correlator. The missing frequencies here are

12	489.924 229
16	2604.597 168
17	2574.601 807.

The second of these was detected but was not listed. The first was not detected. The third frequency was apparently shifted into the region covered by the most predominant frequency in the record and was not detected. The apparently spurious frequencies in this list are

609.905 670

314.951 290

579.910 309.

However, examination of the power spectrum computed in the standard case shows that these frequencies were all detected there, but were not listed due to their low energy content. Hence, these are not at all spurious.

Table 2.6 lists the "predominant" frequencies as compiled by RAVAN modified to compute a completely clipped power spectrum from the standard autocorrelation function. The missing frequencies are

7	419.935 055
12	489.924 229
14	504.921 909
15	404.937 374
16	2604.597 168
17	2574.601 807
19	2539.607 239.

A careful scrutiny of this power spectrum, however, shows that all save the second of these were detected, but were not listed due to the garbling of amplitudes. The second was detected 484.924 229 but was not listed for the same reason.. The apparently spurious frequencies in this list are

1489.769 592
2209.658 264
2444.621 918
109.982 990
1389.785 065
884.863 152
824.872 429.

An examination of the power spectrum computed in the standard case shows that all of these frequencies save the second correspond to minor peaks which were detected but not listed due to their weak energy content. The second of these frequencies appears to be completely spurious.

Table 2.7 lists the predominant frequencies as compiled by RAVAN modified to compute a completely clipped power spectrum

from a polarity coincidence correlator. The missing frequencies here are

4	384.940 468
11	674.895 622
12	489.924 229
14	504.921 909
16	404.937 374
17	2604.597 168

where the integers refer to the numbering of these frequencies in the standard case. An examination of the power spectrum computed in this case shows that all save the third of these were detected but not listed due to the garbling of amplitudes. The fifth and seventh frequencies above were detected as 399.938 and 2579.600 respectively, this being a shift of magnitude $\Delta\omega$ in each case. The apparently spurious frequencies in this table are

164.974 485
609.905 670
2759.573 212
2209.658 264
1474.771 912
2784.569 336
314.951 290.

An examination of the power spectrum computed in the standard case shows that all save the fifth and sixth of these

correspond to frequencies detected in the standard case but not listed because of their low energy content. The fifth appears to be entirely spurious, while the sixth may very well be a second detection of the frequency 2759.573 212.

CROSS REFERENCE TO TABLES AND FIGURES
MEASUREMENT NUMBER E106-11

Table	Functions	Figures
1.1	STANDARD ACF AND PSD	1.10 - 1.13
1.2	STANDARD ACF AND COSINE-CLIPPED PSD	1.21 - 1.22
1.3	HALF-POLARITY CORRELATOR AND STANDAR PSD	1.31 - 1.33
1.4	HALF-POLARITY CORRELATOR AND COSINE-CLIPPED PSD	1.41 - 1.42
1.5	POLARITY COINCIDENCE CORRELATOR AND STANDARD PSD	1.51 - 1.53
1.6	STANDARD ACF AND COMPLETELY CLIPPED PSD	1.61 - 1.62
1.7	POLARITY COINCIDENCE CORRELATOR AND COMPLETELY CLIPPED PSD	~~1.71 - 1.72~~

MEASUREMENT NUMBER L63-11

2.1	STANDARD ACF AND PSD	2.10 - 2.13
2.2	STANDARD ACF AND COSINE-CLIPPED PSD	2.21 - 2.22
2.3	HALF-POLARITY CORRELATOR AND STANDARD PSD	2.31 - 2.32
2.4	HALF POLARITY CORRELATOR AND COSINE-CLIPPED PSD	2.41 - 2.42
2.5	POLARITY COINCIDENCE CORRELATOR AND STANDARD PSD	2.51 - 2.53
2.6	STANDARD ACF AND COMPLETELY CLIPPED PSD	2.61 - 2.62
2.7	POLARITY COINCIDENCE CORRELATOR AND COMPLETELY CLIPPED PSD	2.71 - 2.72

SUMMARY OF EXPERIMENTAL RESULTS; RECOMMENDATIONS

We have observed that in all instances where the clipping technique has been applied to the problem of frequency determination, the results have been (1) a garbling of the order of predominance of data frequencies, and (2), a loss of all information concerning the amplitude of a given frequency. One exception to this rule is that, of the four records analyzed, the "most predominant" frequency was always listed as such, regardless of the severity of clipping. This suggests that the use of the completely clipped power spectral density function in conjunction with the polarity coincidence correlator may be entirely adequate in many applications where the determination of this frequency is the only concern.

It is known that the half-polarity correlator is an unbiased estimator of the true correlator when the noise present in the signal is gaussian, and it has been suggested that it may be possible to discover a bias function when the noise is nongaussian. This would be an extremely useful result, for, as shown in the experimental data tables, the cosine-clipped power spectrum is a highly reliable device for determining data frequencies from the standard autocorrelation function, and the use of these two functions together would make possible great savings in machine time, when efficient programming techniques were employed.

Finally, we note that the development of the power spectrum as a series in the cosine-clipped power spectrum can be

carried out by hand to any finite number of terms. Since the energy at high frequencies is known to be negligible in many situations, this raises the possibility of recovering the amplitude of the power spectrum at a given frequency from the amplitudes of the cosine-clipped spectrum. This, however, is at present only a theoretical possibility, and will require experimental verification.

REFERENCES

(1) Blackman, R. B. and J. W. Tukey, "The Measurement of Power Spectra from the Point of View of Communications Engineering". Dover Publications, 1959.

(2) N. D. Diamantides, "Analog Technique Deriver Correlation Functions". Electronics, April, 1962.

(3) P. D. Welch, "A Direct Method of Power Spectrum Estimation." IBM Jour., April., 1961.

(4) H. S. Tsien, "Engineering Cybernetics". McGraw-Hill (1954).

MEASUREMENT NUMBER E106-11

STANDARD AUTOCORRELATION AND POWER SPECTRAL DENSITY FUNCTION.

Number	Predominant Frequencies	RMS Amplitudes
1	365.056 950	0.662 608
2	325.050 709	0.633 961
3	1075.167 725	0.615 877
4	1030.160 706	0.587 619
5	1015.158 371	0.585 167
6	500.078 014	0.580 636
7	300.046 810	0.579 561
8	990.154 472	0.530 216
9	480.074 894	0.515 191
10	720.112 343	0.511 810
11	345.053 829	0.508 324
12	545.085 037	0.503 209
13	525.081 917	0.499 861
14	1105.172 409	0.495 931
15	640.099 861	0.489 179
16	1045.163 055	0.487 745
17	1115.173 965	0.480 162
18	930.145 111	0.471 739
19	95.014 823	0.461 133
20	275.042 908	0.433 540

Table 1.1

MEASUREMENT NUMBER E106-11

HALF-POLARITY CORRELATOR AND STANDARD POWER SPECTRAL DENSITY FUNCTION

Number	"Predominant" Frequencies	RMS "Amplitudes"
1	365.056 950	0.274 696
(3)	1070.166 946	0.265 311
(2)	320.049 931	0.255 968
4	1030.160 706	0.250 931
7	300.046 810	0.245 287
(6)	495.077 236	0.240 695
9	480.074 894	0.237 287
5	1015.158 371	0.235 781
13	525.081 917	0.232 938
(12)	540.084 251	0.226 340
(8)	980.152 908	0.217 750
16	1045.163 055	0.215 778
17	1115.173 965	0.215 523
	705.110 001	0.214 853
(10)	715.111 557	0.213 296
19	95.014 823	0.211 458
14	1105.172 409	0.207 819
11	345.053 829	0.207 774
	935.145 889	0.204 747
	555.086 594	0.200 861

Table 1.2

MEASUREMENT NUMBER E106-11

STANDARD AUTOCORRELATION FUNCTION AND COSINE-CLIPPED POWER SPECTRAL DENSITY FUNCTION

Number	"Predominant" Frequencies	RMS "Amplitudes"
1	365.056 950	0.720 457
3	1075.167 725	0.683 412
6	500.078 014	0.661 923
5	1015.158 371	0.661 845
4	1030.160 706	0.654 330
2	325.050 709	0.631 623
9	480.074 894	0.588 696
7	300.046 810	0.580 915
10	720.112 343	0.577 996
8	990.154 472	0.572 586
13	525.081 917	0.567 329
16	1045.163 055	0.556 964
15	640.099 861	0.554 362
17	1115.173 965	0.552 092
14	1105.172 409	0.542 657
12	545.085 037	0.533 041
18	930.145 111	0.507 720
	735.114 677	0.495 006
	845.131 844	0.492 438
	790.123 260	0.491 584

Table 1.3

MEASUREMENT NUMBER E106-11

HALF POLARITY CORRELATOR AND COSINE-CLIPPED POWER SPECTRAL DENSITY FUNCTION

Number	"Predominant" Frequencies	RMS "Amplitudes"
1	365.056 950	.297 788
(3)	1070.166 946	.202 682
4	1030.160 706	.279 666
9	480.074 894	.271 477
(6)	495.077 236	.270 839
(2)	320.049 931	.267 831
5	1015.158 371	.266 737
13	525.081 917	.262 425
7	300.046 810	.259 983
(12)	540.084 251	.243 598
17	1115.173 965	.243 520
	705.110 001	.242 482
16	1045.163 055	.241 852
(10)	715.111 557	.238 849
(8)	980.152 908	.228 149
15	640.099 861	.226 079
(18)	935.145 889	.224 096
	555.086 594	.223 229
	735.114 677	.218 393
	1000.156 029	.215 940

Table 1.4

MEASUREMENT NUMBER E106-11

POLARITY COINCIDENCE CORRELATOR AND STANDARD POWER SPECTRAL DENSITY FUNCTION.

Number	"Predominant" Frequencies	RMS "Amplitudes"
1	365.056 950	0.126 049
(3)	1070.166 946	.119 632
2	325.050 709	.115 940
5	1015.158 371	.111 969
13	525.081 917	.110 165
4	1030.160 706	.108 995
9	480.074 894	.107 752
	555.086 594	.107 024
(12)	540.084 251	.105 500
(7)	310.048 370	.103 720
11	345.053 829	.102 982
19	95.014 823	.101 592
17	1115.173 965	.101 295
6	500.078 014	.099 305
16	1045.163 055	.097 942
(10)	715.111 557	.097 239
(18)	940.146 667	.096 432
(9)	975.152 130	.096 242
15	640.099 861	.093 326
	705.110 001	.092 384

Table 1.5

MEASUREMENT NUMBER E106-11

STANDARD AUTOCORRELATION FUNCTION AND COMPLETELY CLIPPED POWER SPECTRAL DENSITY FUNCTION.

Number	"Predominant" Frequencies	RMS "Amplitudes"
1	365.056 950	1.508 127
	790.123 260	1.490 305
3	1075.167 725	1.489 361
2	325.050 709	1.461 723
6	500.078 014	1.461 723
	1580.246 521	1.461 723
15	640.099 861	1.460 761
17	1115.173 965	1.454 006
(8)	975.152 130	1.453 039
4	1030.160 706	1.453 039
10	715.111 557	1.450 132
18	930.145 111	1.449 162
5	1015.158 371	1.448 192
	215.033 546	1.446 248
19	95.014 823	1.444 302
13	525.081 917	1.442 354
	2030.316 742	1.442 354
7	300.046 810	1.439 426
(12)	540.084 251	1.439 426
	625.097 519	1.439 426

Table 1.6

MEASUREMENT NUMBER E106-11

POLARITY COINCIDENCE CORRELATOR AND COMPLETELY CLIPPED POWER SPECTRAL DENSITY FUNCTION

Number	"Predominant" Frequencies	RMS "Amplitudes"
1	365.056 950	1.483 977
19	95.014 823	1.465 862
(3)	1070.166 946	1.464 902
	1580.246 521	1.459 131
	790.123 260	1.456 237
17	1115.173 965	1.452 369
9	480.074 894	1.452 369
11	345.053 829	1.451 400
4	1030.160 706	1.450 431
15	640.099 861	1.450 431
5	1015.158 371	1.447 520
13	220.034 327	1.446 548
(2)	525.081 917	1.446 548
	320.049 931	1.445 575
	735.114 677	1.444 602
	555.086 594	1.443 628
18	975.152 130	1.441 679
	930.145 111	1.439 727
	3160.493 042	1.438 750
	770.120 140	1.437 772

Table 1.7

MEASUREMENT NUMBER L63-11

STANDARD AUTOCORRELATOR AND POWER SPECTRAL DENSITY FUNCTION

Number	Predominant Frequencies	RMS Amplitudes
1	2559.604 126	0.158 678
2	529.918 045	0.125 367
3	354.945 107	0.111 290
4	384.940 468	0.110 900
5	234.963 661	0.109 705
6	269.958 248	0.108 419
7	419.935 055	0.104 882
8	444.931 190	0.102 129
9	299.953 609	0.098 289
10	549.914 948	0.097 904
11	674.895 622	0.093 245
12	489.924 229	0.090 037
13	979.848 457	0.088 407
14	504.921 909	0.087 202
15	404.937 374	0.086 351
16	2604.597 168	0.086 136
17	2574.601 807	0.085 964
18	939.854 645	0.084 922
19	2539.607 239	0.084 261
20	1109.828 354	0.082 690

Table 2.1

MEASUREMENT NUMBER L63-11

STANDARD AUTOCORRELATOR AND COSINE-CLIPPED POWER SPECTRAL DENSITY FUNCTION

Number	"Predominant" Frequencies	RMS "Amplitudes"
1	2559.604 126	0.177 275
2	529.918 045	0.144 956
8	444.931 190	0.121 465
3	354.945 107	0.120 676
4	384.940 468	0.117 681
10	549.914 948	0.117 067
6	269.958 248	0.114 662
5	234.963 661	0.114 048
	454.929 642	0.111 125
7	419.935 055	0.110 487
	3159.511 353	0.103 933
(13)	984.847 687	0.103 607
14	504.921 909	0.103 446
9	299.953 609	0.102 092
12	489.924 229	0.101 322
17	2574.601 807	0.097 826
11	674.895 622	0.096 826
18	939.854 645	0.093 389
20	1109.828 354	0.091 816
15	404.937 374	0.090 083

Table 2.2

MEASUREMENT NUMBER L63-11

HALF-POLARITY CORRELATOR WITH STANDARD POWER SPECTRAL DENSITY FUNCTION

Number	"Predominant" Frequencies	RMS "Amplitude"
1	2559.604 126	0.138 545
2	529.918 045	0.110 101
7	419.935 055	0.099 110
3	354.945 107	0.097 319
5	234.963 661	0.095 111
6	269.958 248	0.094 268
9	299.953 609	0.093 459
10	549.914 948	0.090 395
4	384.940 468	0.089 699
(8)	439.931 961	0.089 614
11	674.895 622	0.083 656
(13)	984.847 687	0.081 604
15	404.937 374	0.081 057
(14)	499.922 684	0.080 189
12	489.924 229	0.077 682
19	2539.607 239	0.077 563
	614.904 900	0.076 108
	454.929 642	0.075 987
18	939.854 647	0.075 116
20	1109.828 354	0.074 440

Table 2.3

MEASUREMENT NUMBER L63-11

HALF-POLARITY CORRELATOR AND COSINE-CLIPPED POWER SPECTRUM

Number	"Predominant" Frequencies	RMS "Amplitudes"
1	2559.604 126	0.154 819
2	529.918 045	0.126 167
10	549.914 948	0.107 229
(8)	439.931 961	0.106 569
3	354.945 107	0.105 559
7	419.935 055	0.105 202
6	269.958 248	0.100 374
5	234.963 661	0.097 038
9	299.953 609	0.097 026
(13)	984.847 687	0.095 578
(14)	499.922 684	0.094 551
4	384.940 468	0.093 870
	454.929 642	0.091 161
	3159.511 353	0.088 612
11	674.895 622	0.087 771
15	404.937 374	0.087 332
12	489.924 229	0.085 952
(19)	2544.606 445	0.084 018
20	1109.828 354	0.083 844
	2659.588 684	0.083 372

Table 2.4

MEASUREMENT NUMBER L63-11

POLARITY COINCIDENCE CORRELATOR AND STANDARD POWER SPECTRAL DENSITY FUNCTION

Number	"Predominant" Frequency	RMS "Amplitudes"
1	2559.604 126	0.123 687
2	529.918 045	0.099 025
9	299.953 609	0.095 213
7	419.935 055	0.095 113
5	234.963 661	0.090 861
(6)	264.959 023	0.090 778
3	354.945 107	0.090 131
10	549.914 948	0.088 252
8	444.931 190	0.087 748
4	384.940 468	0.086 571
(19)	2544.606 445	0.085 411
13	979.848 457	0.085 052
15	404.937 374	0.084 021
	609.905 670	0.081 748
11	674.895 622	0.080 468
	314.951 290	0.077 297
(18)	934.855 423	0.077 207
14	504.921 909	0.076 593
	579.910 309	0.075 412
20	1114.827 576	0.074 269

Table 2.5

MEASUREMENT NUMBER L63-11

Number	"Predominant" Frequencies	RMS "Amplitudes"
1	2559.604 126	1.571 235
2	529.918 045	1.479 321
3	354.945 107	1.450 711
9	299.953 609	1.447 719
6	269.958 248	1.444 721
5	234.963.661	1.442 719
4	384.940 468	1.441 716
8	444.931 190	1.441 716
	1489.769 592	1.439 710
(13)	984.847 687	1.437 701
	2209.658 264	1.436 695
20	1109.828 354	1.435 689
11	674.895 622	1.432 666
10	549.914 948	1.431 656
(18)	934.855 423	1.431 656
	2444.621 918	1.431 656
	109.982 990	1.430 646
	1389.785 065	1.430 646
	884.863 152	1.427 613
	824.872 429	1.427 613

Table 2.6

MEASUREMENT NUMBER L63-11

Number	"Predominant" Frequencies	RMS "Amplitudes"
1	2559.604 126	1.513 067
7	419.935 055	1.436 629
2	529.918 045	1.434 615
8	444.931 190	1.431 590
9	299.953 609	1.429 569
13	979.848 457	1.429 569
10	549.914 948	1.428 558
(19)	2544.606 445	1.428 558
(20))	1114.827 576	1.426 533
3	354.945 107	1.424 505
	164.974 485	1.421 458
5	234.963 661	1.420 441
	609.905 670	1.418 405
6	269.958 248	1.416 365
	2759.573 212	1.416 365
	2209.658 264	1.412 278
	1474.771 912	1.411 254
	2784.569 336	1.411 254
	314.951 290	1.410 229
(18)	934.855 423	1.410 229

Table 2.7

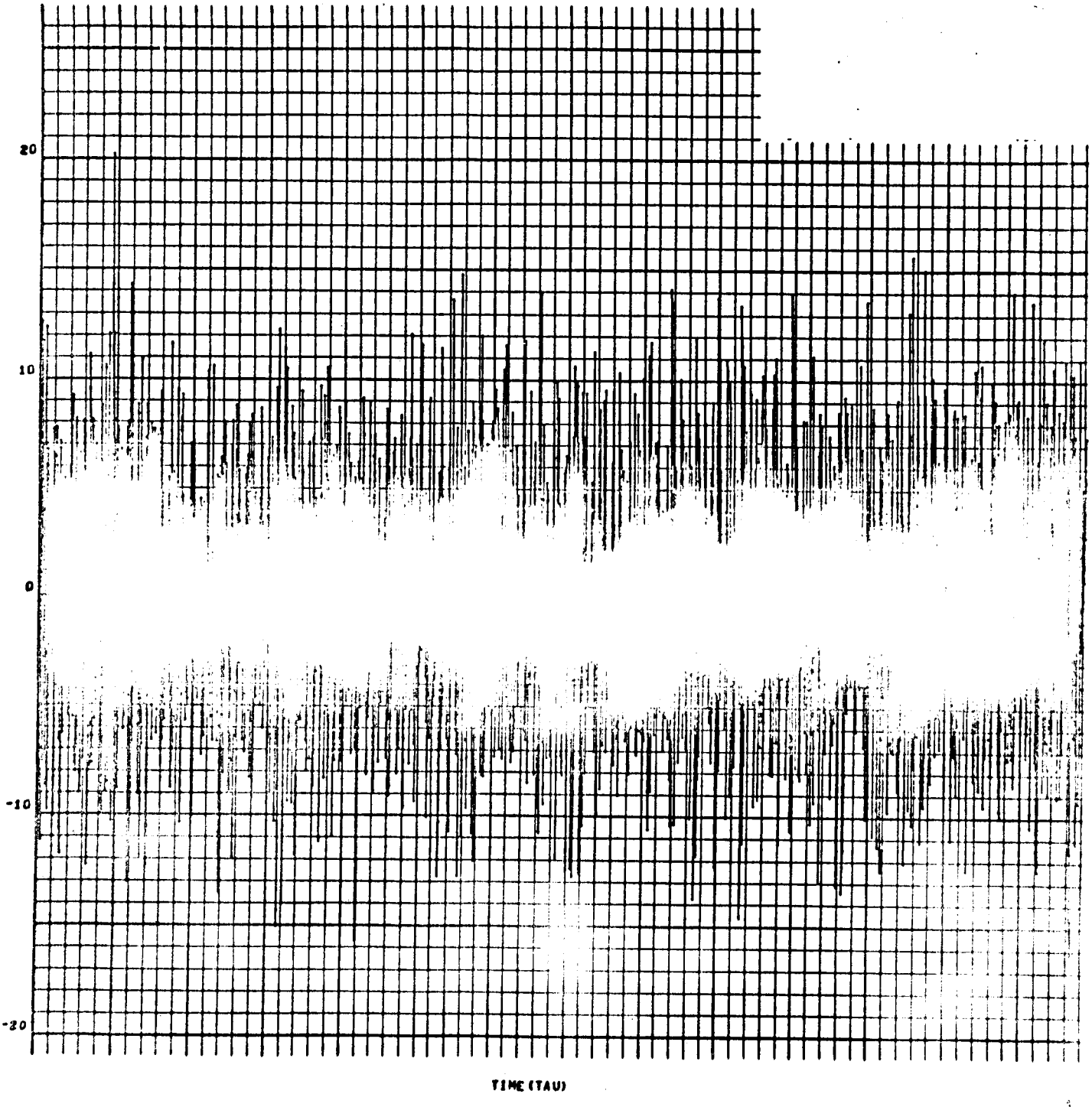

Figure 1.10

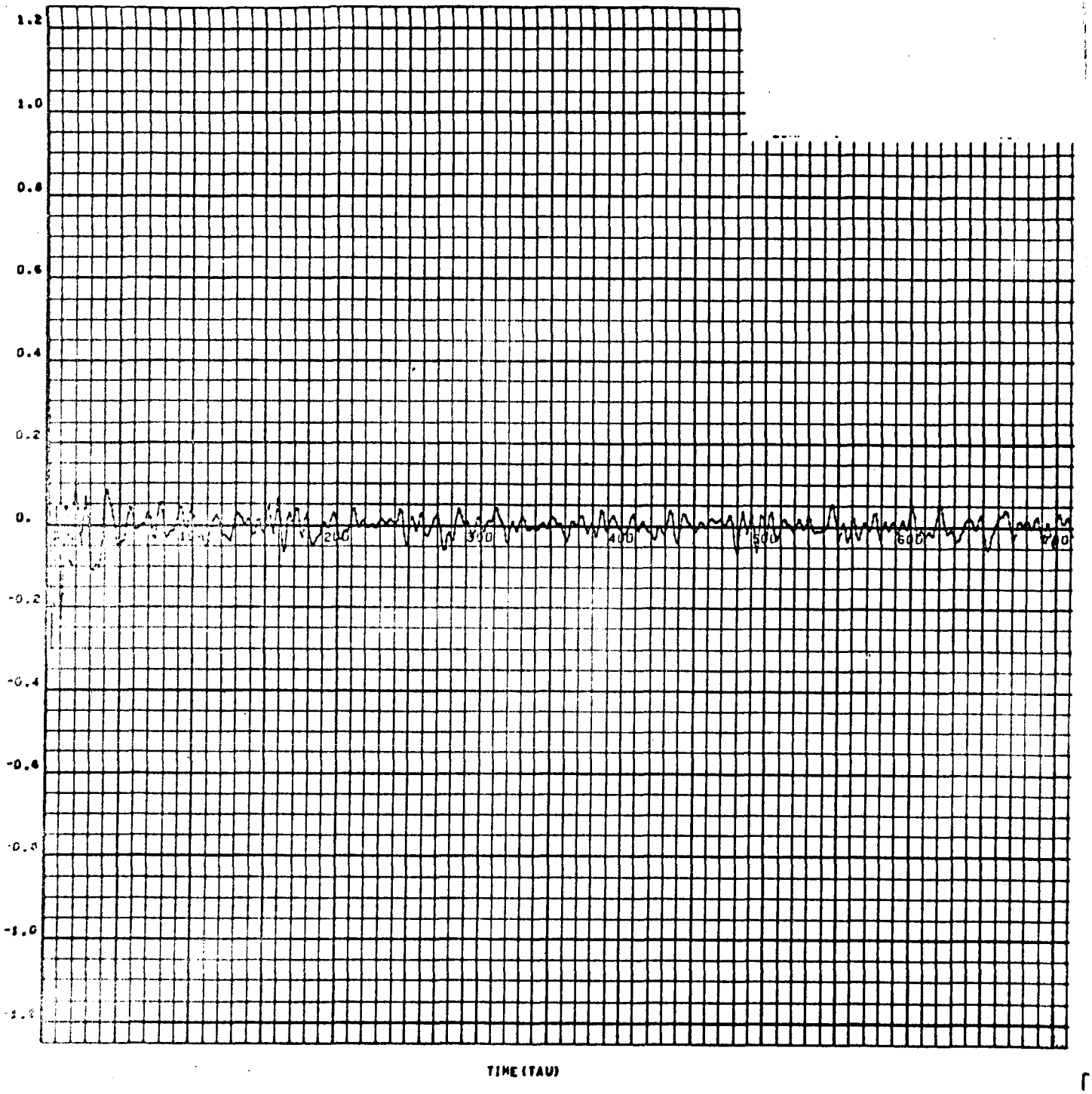

Figure 1.1

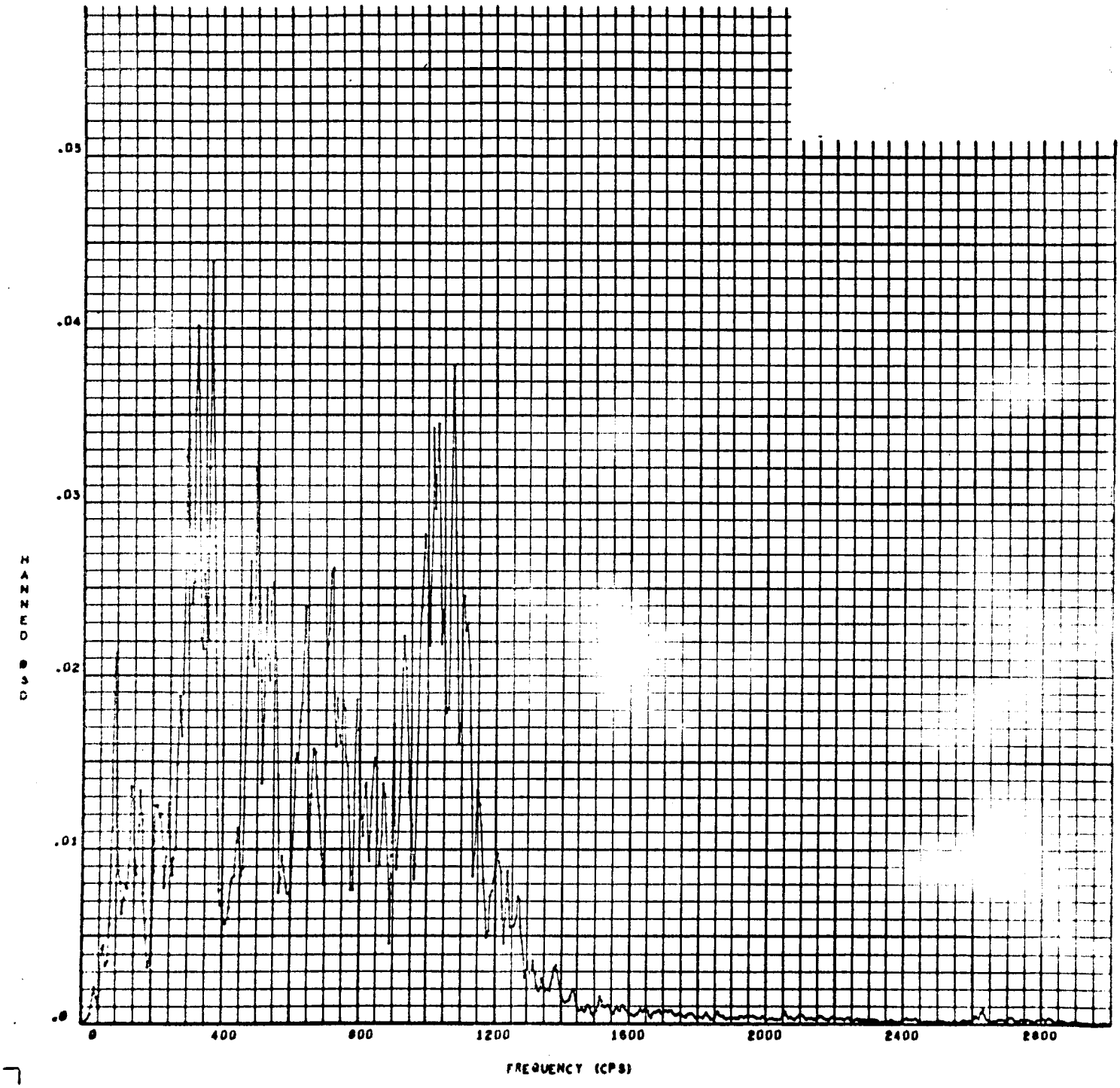
.05
.04
.03
.02
.01
.0
HANNED PSD
0
400
800
1200
1600
2000
2400
2800
FREQUENCY (CPS)

Figure 1.22

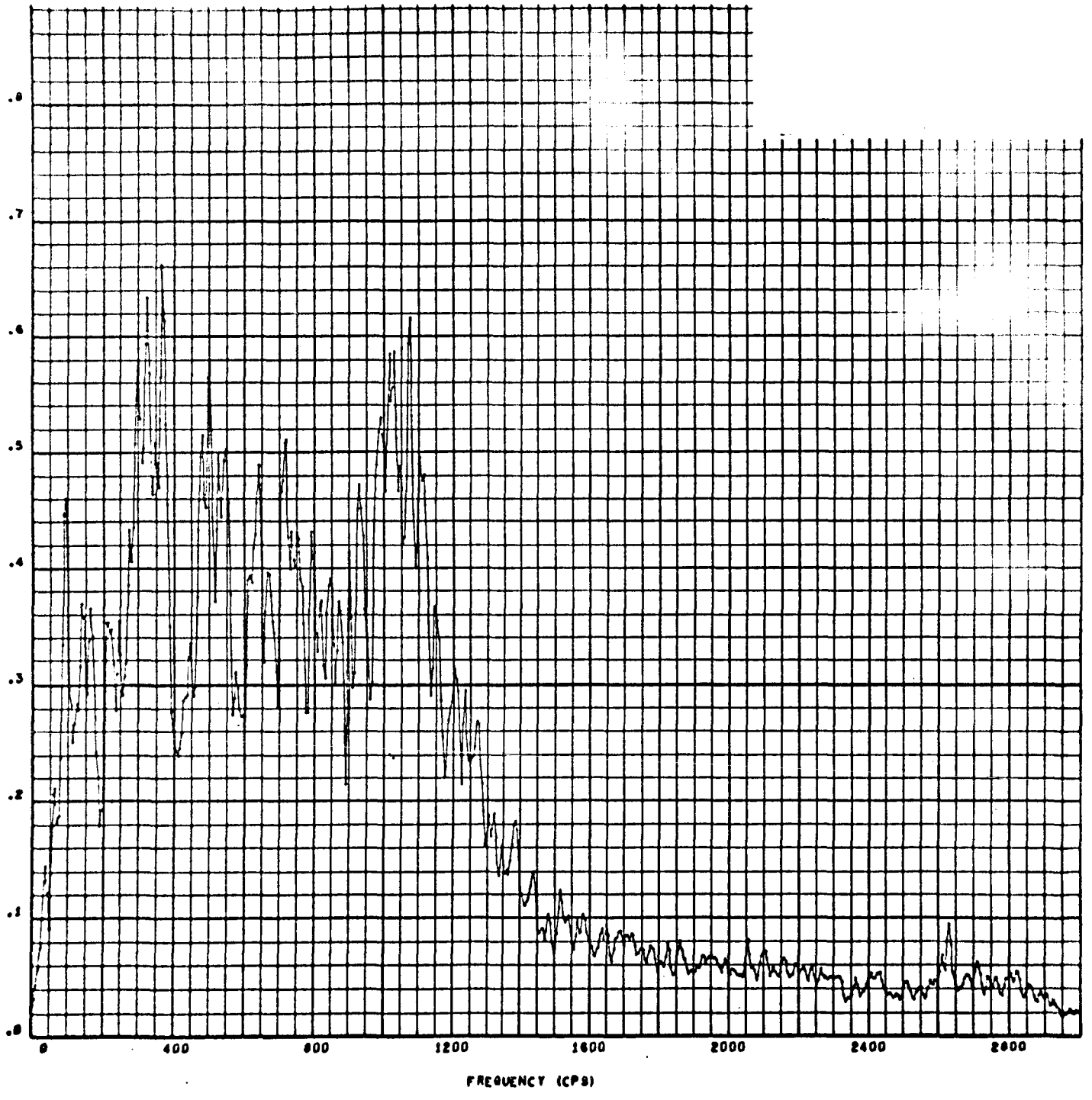
.8
.7
.6
.5
.4
.3
.2
.1
0
RMS AMPLITUDE
0
400
800
1200
1600
2000
2400
2800
FREQUENCY (CPS)

Figure 8.13

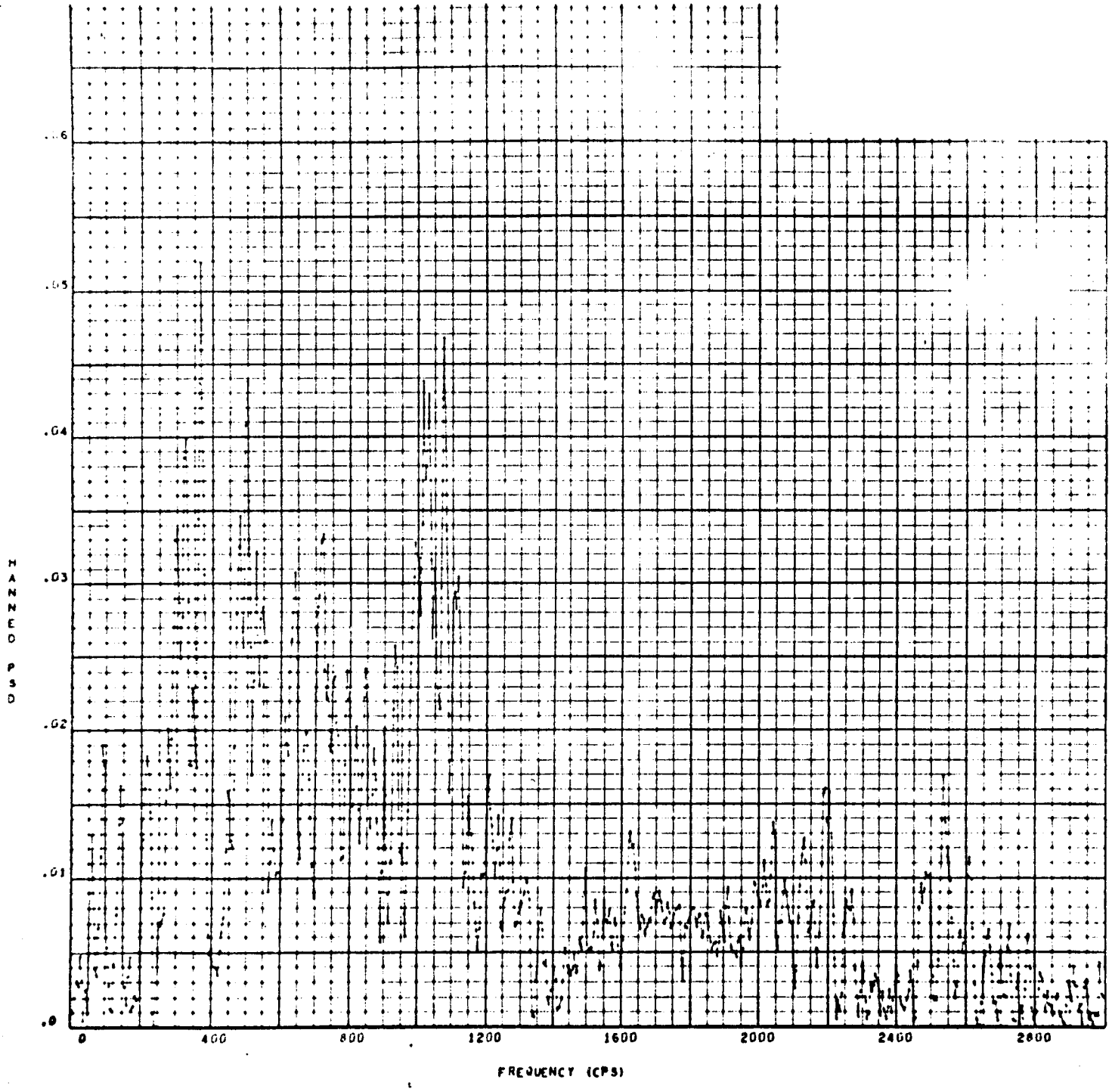
.06
.05
.04
.03
.02
.01
.0
MANNED PSD
0
400
800
1200
1600
2000
2400
2800
FREQUENCY (CPS)

FIGURE 1.21

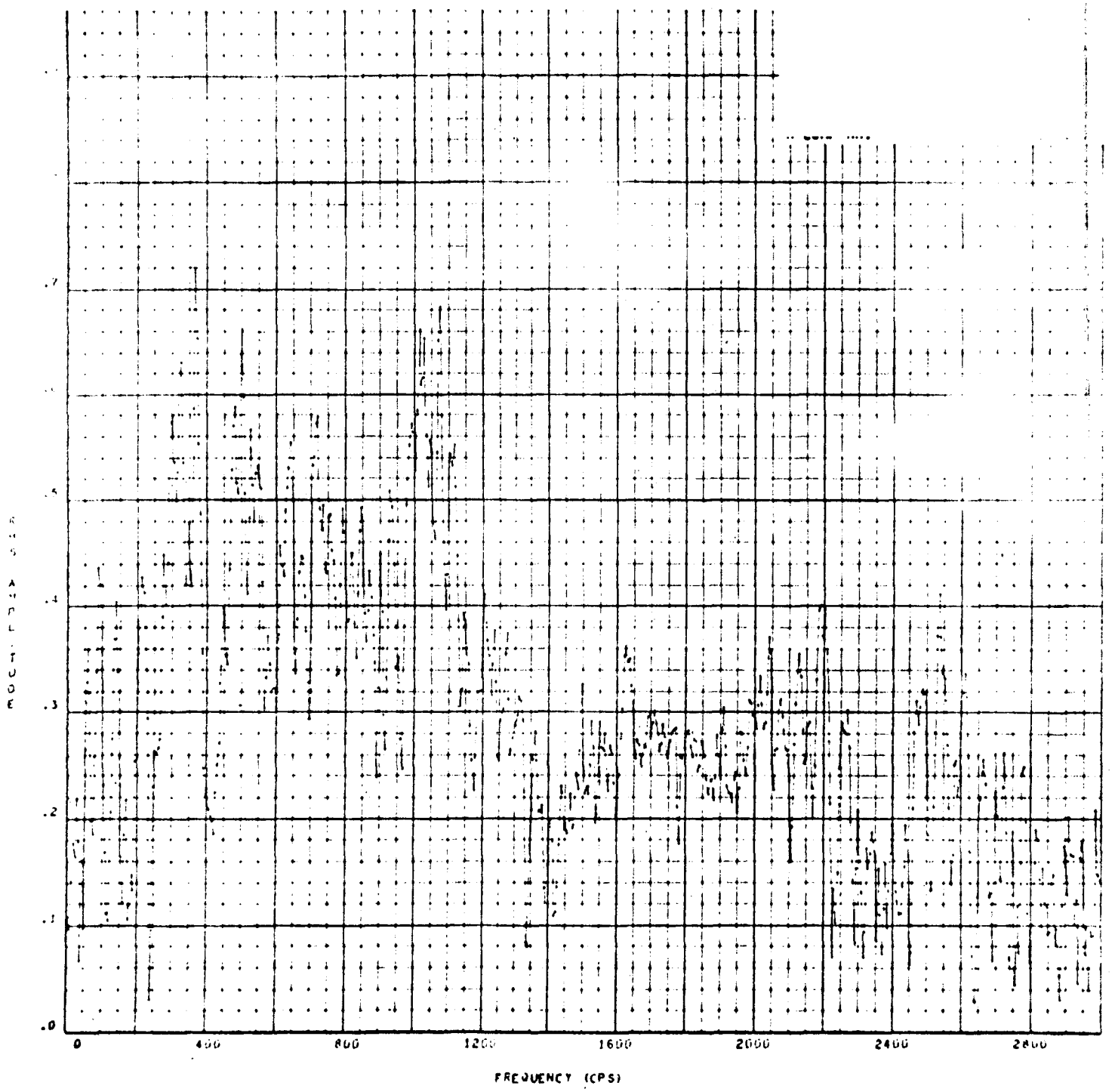

FIGURE 1.22

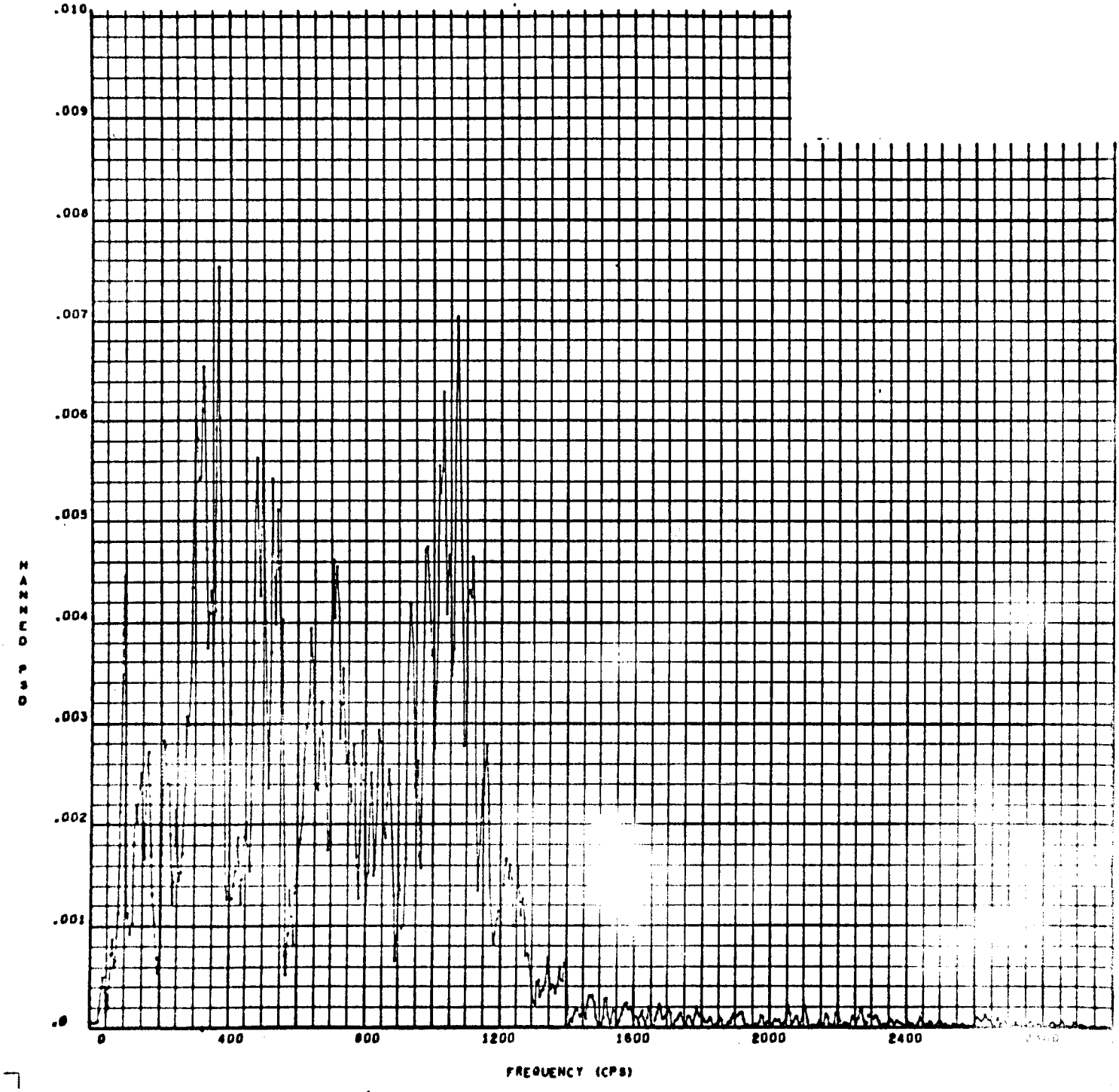
.010
.009
.008
.007
.006
.005
.004
.003
.002
.001
.0
MANNED PSD
0
400
800
1200
1600
2000
2400
FREQUENCY (CPS)

FIGURE 1.31

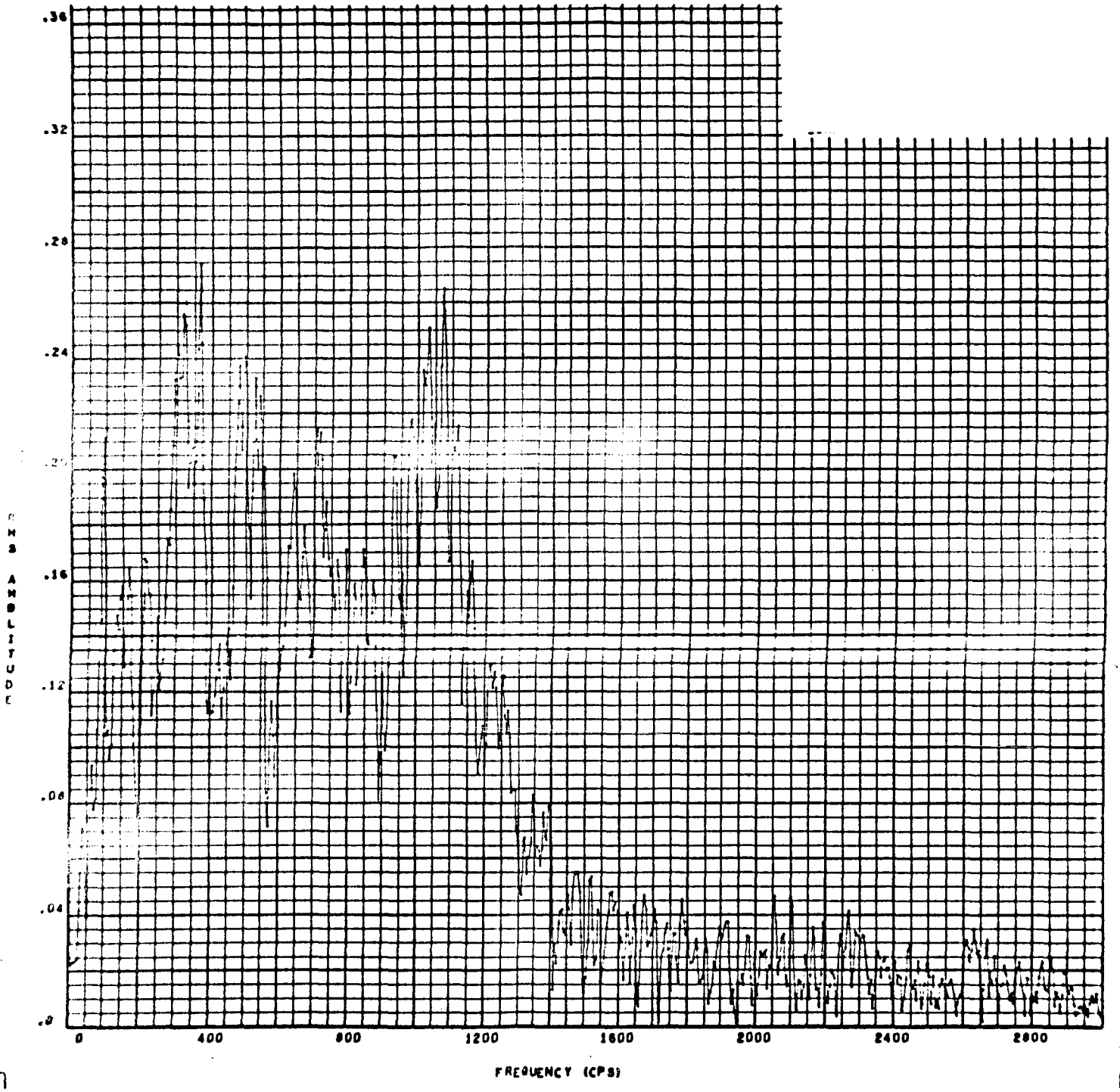
.36
.32
.28
.24
.16
.12
.08
.04
0
400
800
1200
1600
2000
2400
2800
RMS AMPLITUDE
FREQUENCY (CPS)

FIGURE 1.32

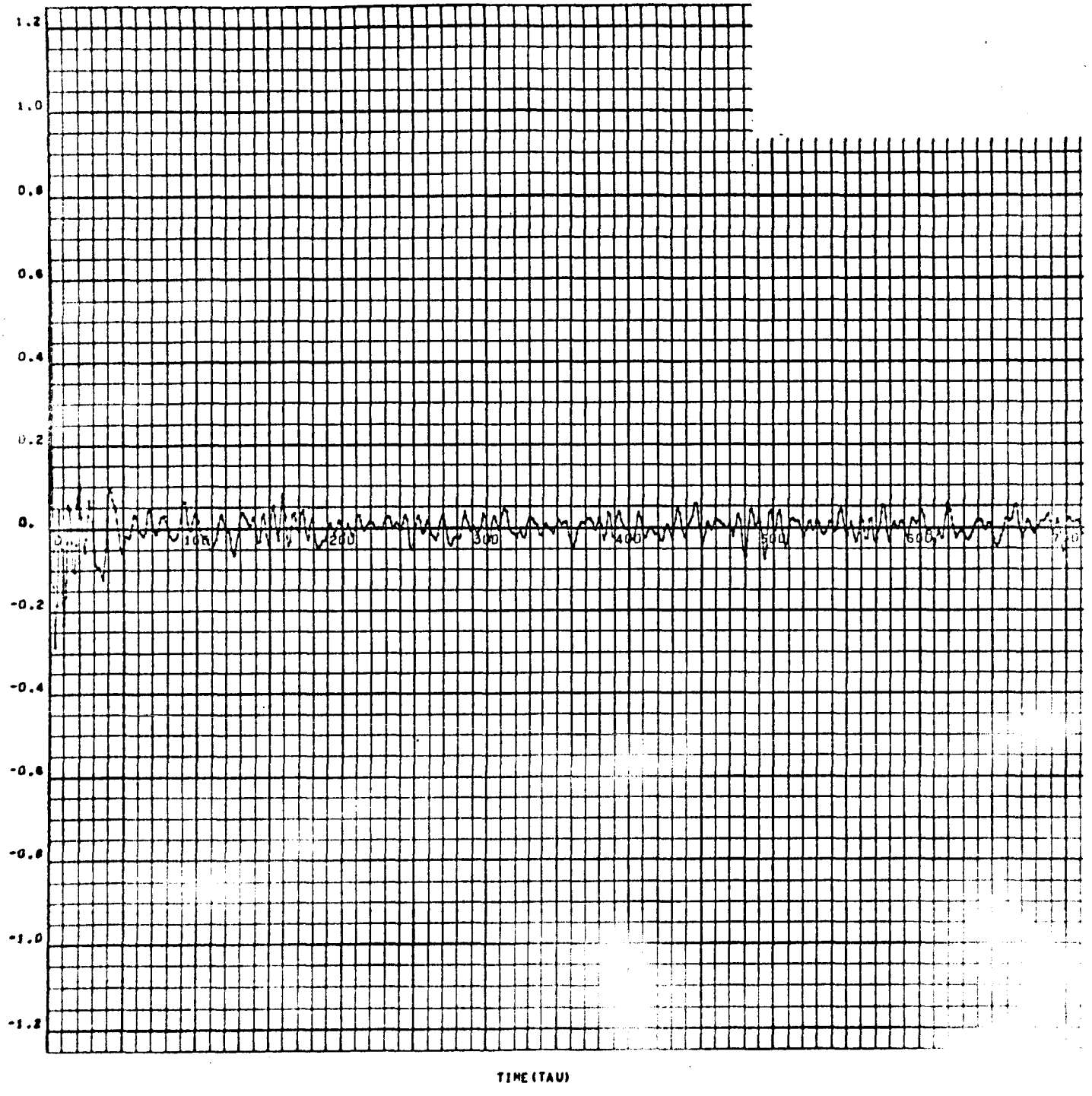
1.2
1.0
0.8
0.6
0.4
0.2
0.
-0.2
-0.4
-0.6
-0.8
-1.0
-1.2
AUTOCORRELATION
100
200
300
400
500
600
TIME (TAU)

FIGURE 1.33

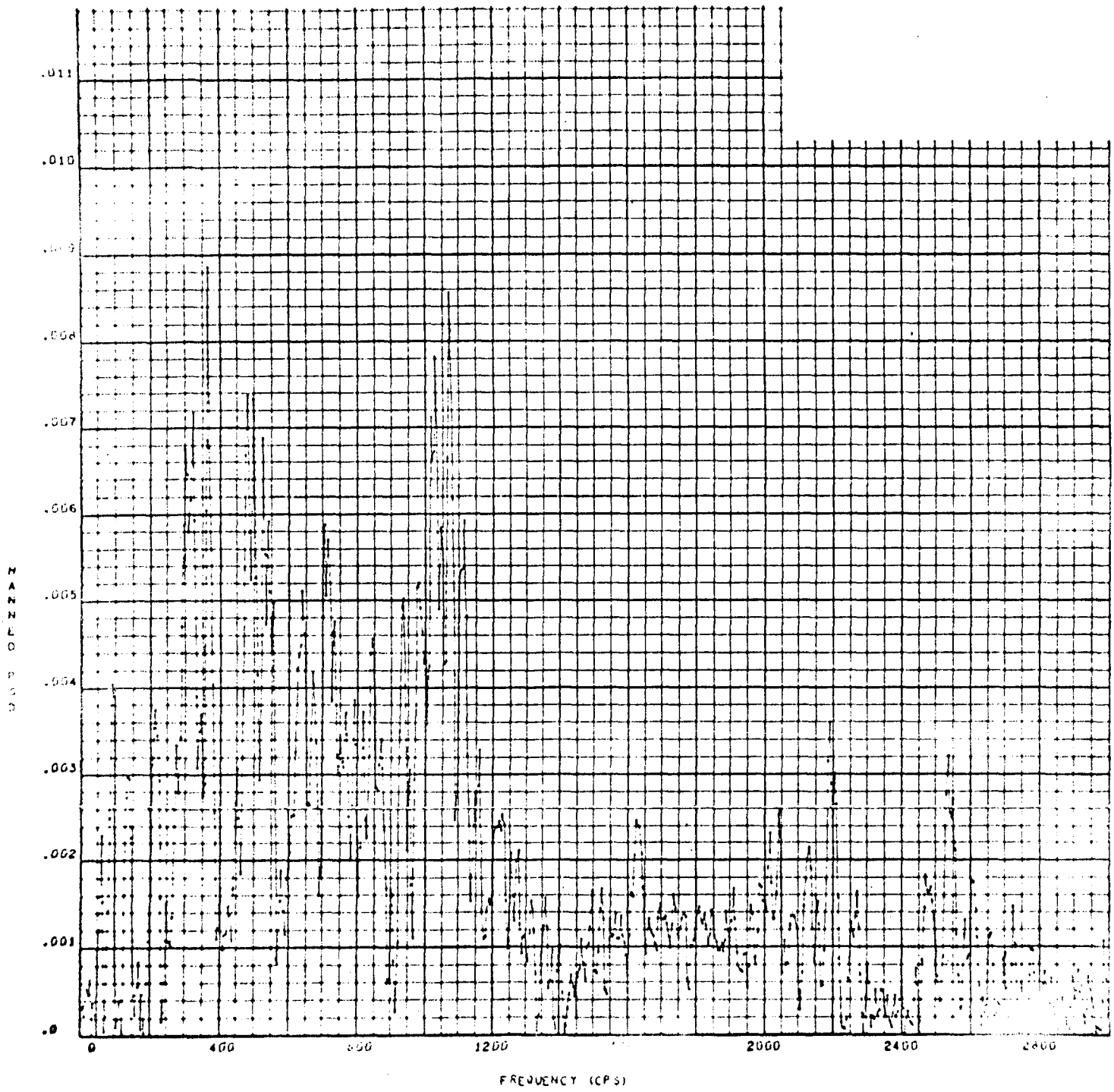
.011
.010
.008
.007
.006
.005
.004
.003
.002
.001
.0
0
400
800
1200
2000
2400
2800
FREQUENCY (CPS)

FIGURE 1.41

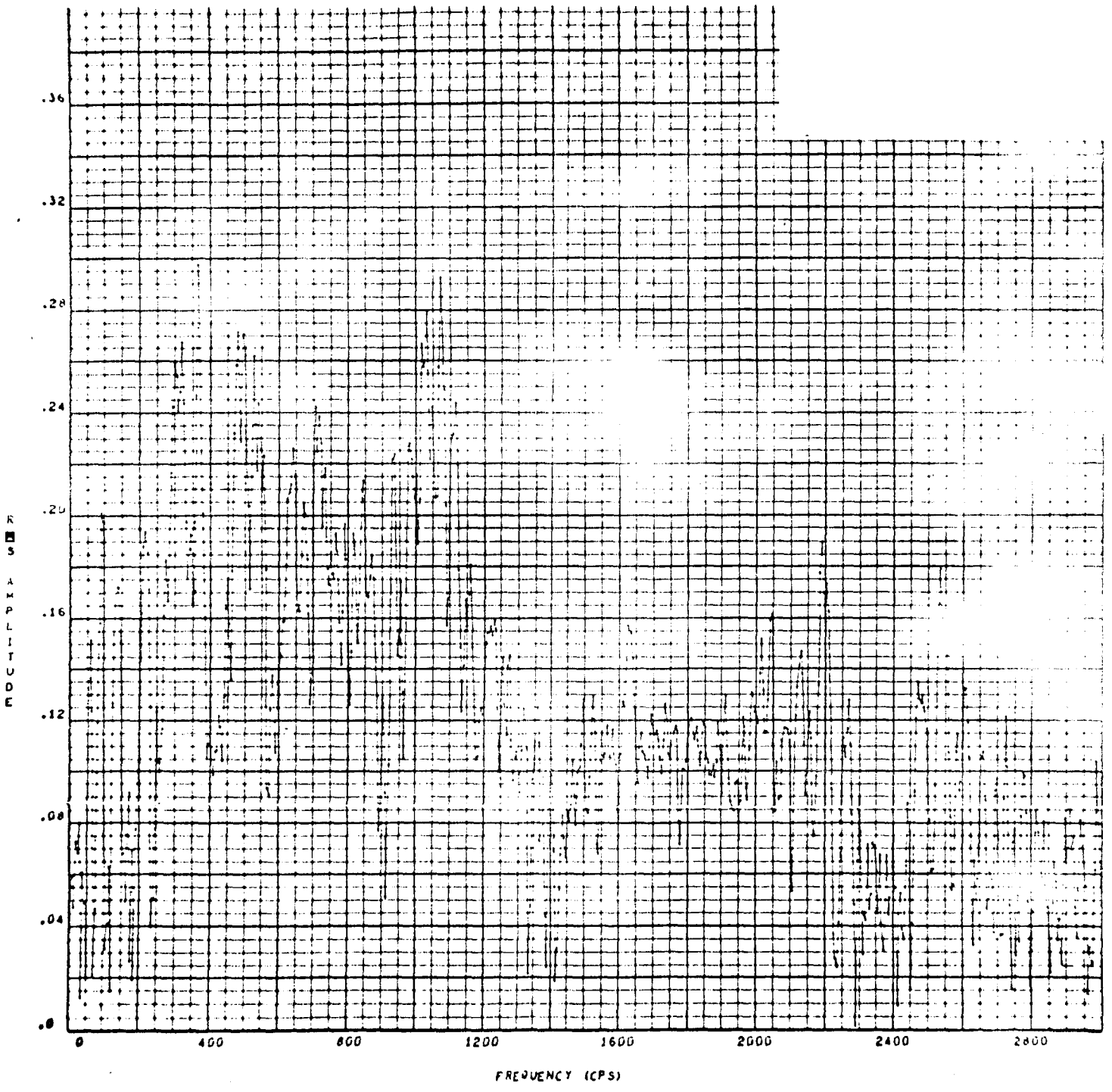
.36
.32
.28
.24
.20
.16
.12
.08
.04
.0
RMS AMPLITUDE
0
400
800
1200
1600
2000
2400
2800
FREQUENCY (CPS)

FIGURE 1.42

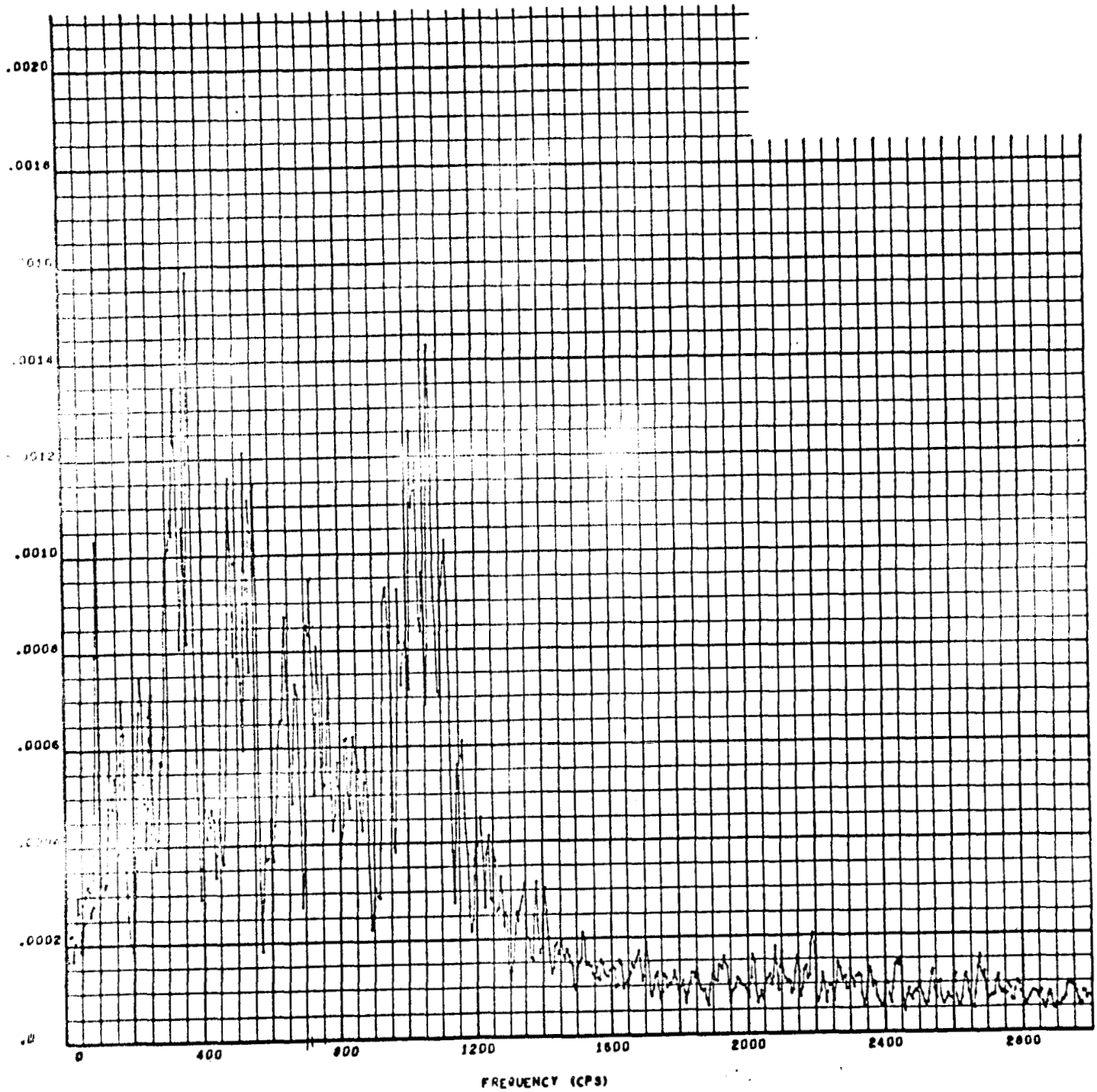
.0020
.0016
.0014
.0010
.0008
.0006
.0002
0
400
800
1200
1600
2000
2400
2800
FREQUENCY (CPS)

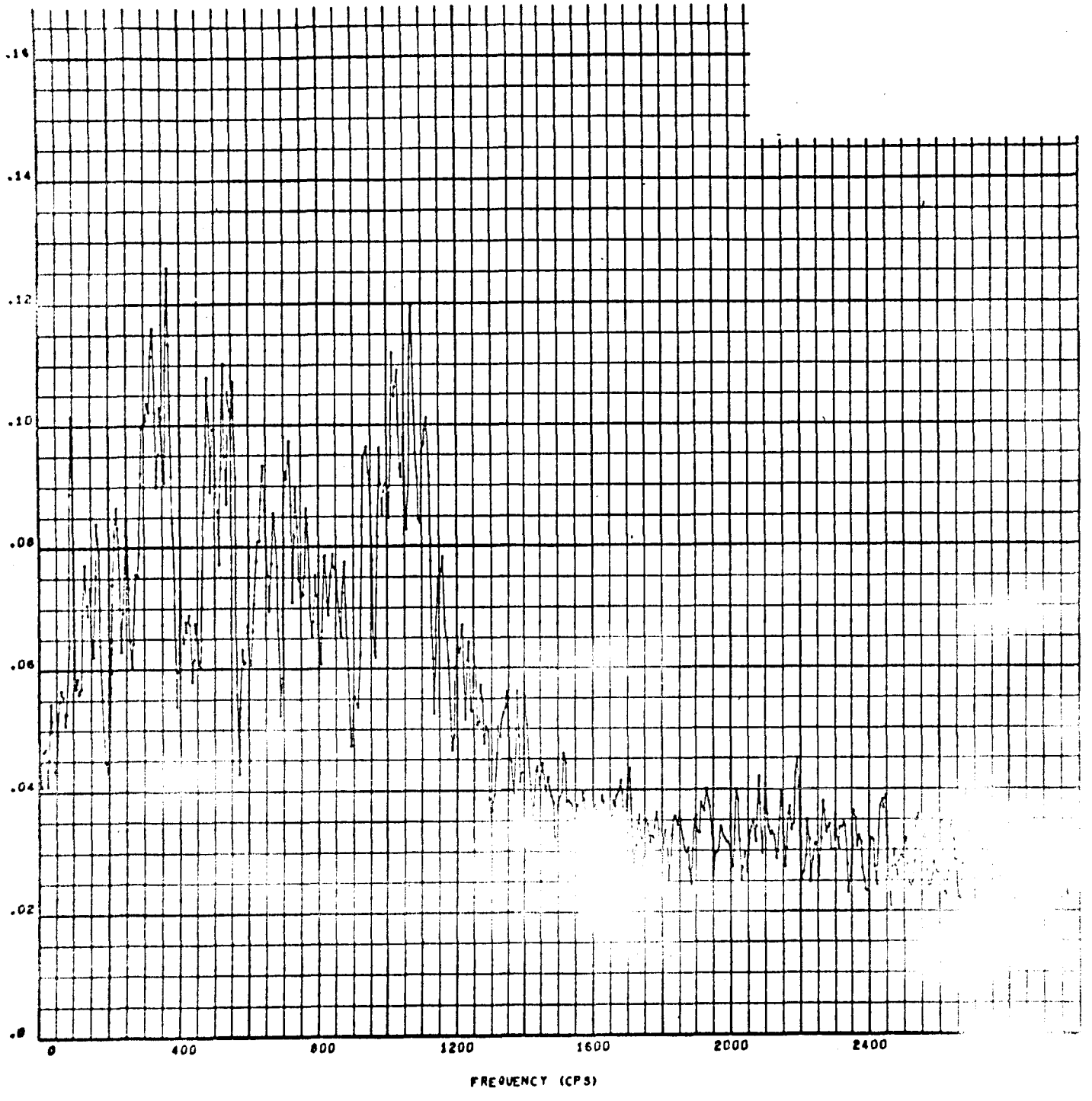
.16
.14
.12
.10
.08
.06
.04
.02
.0
RMS AMPLITUDE
0
400
800
1200
1600
2000
2400
FREQUENCY (CPS)

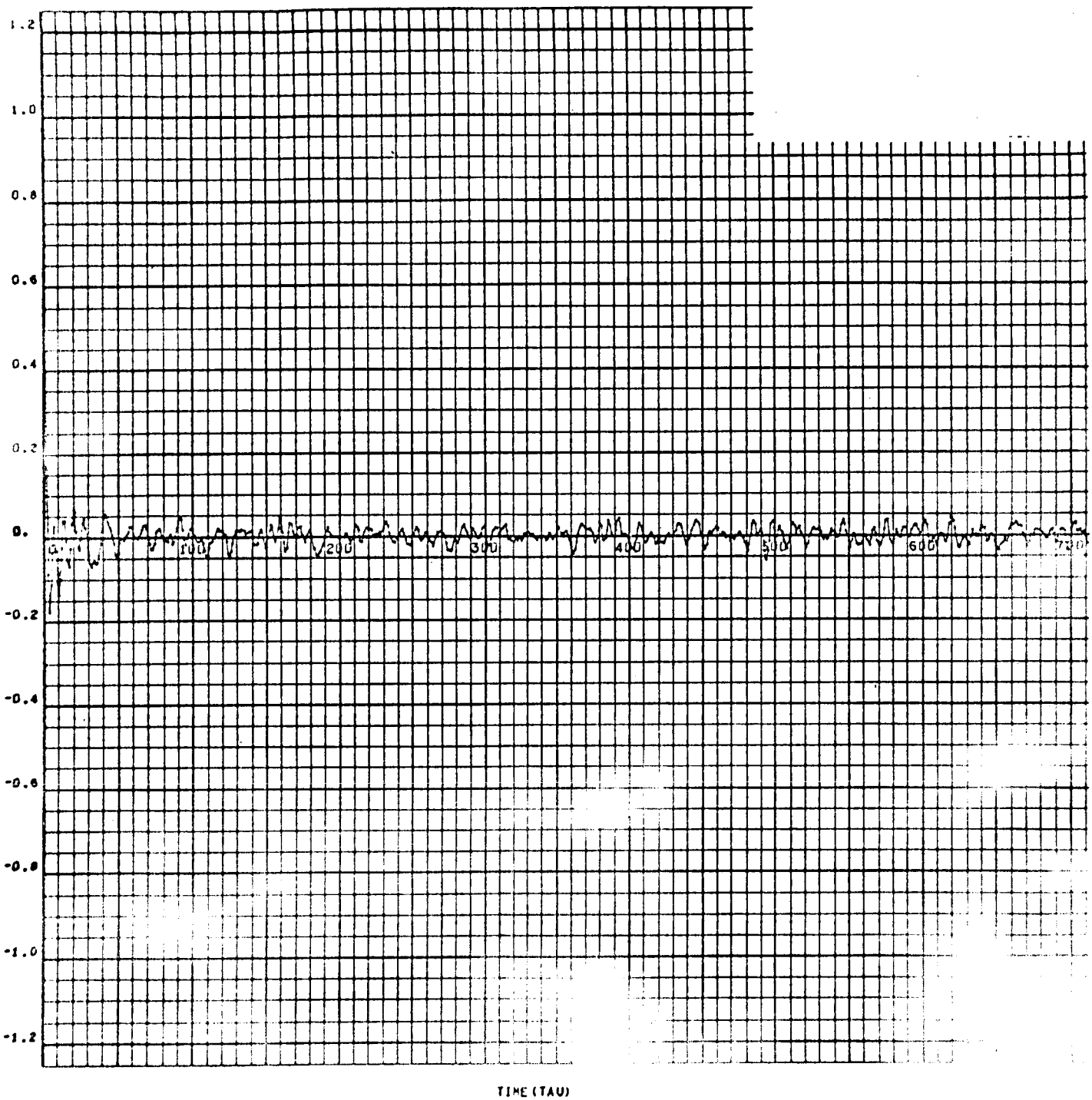
1.2
1.0
0.8
0.6
0.4
0.2
0.
-0.2
-0.4
-0.6
-0.8
-1.0
-1.2
100
200
300
400
500
600
AUTOCORRELATION
TIME (TAU)

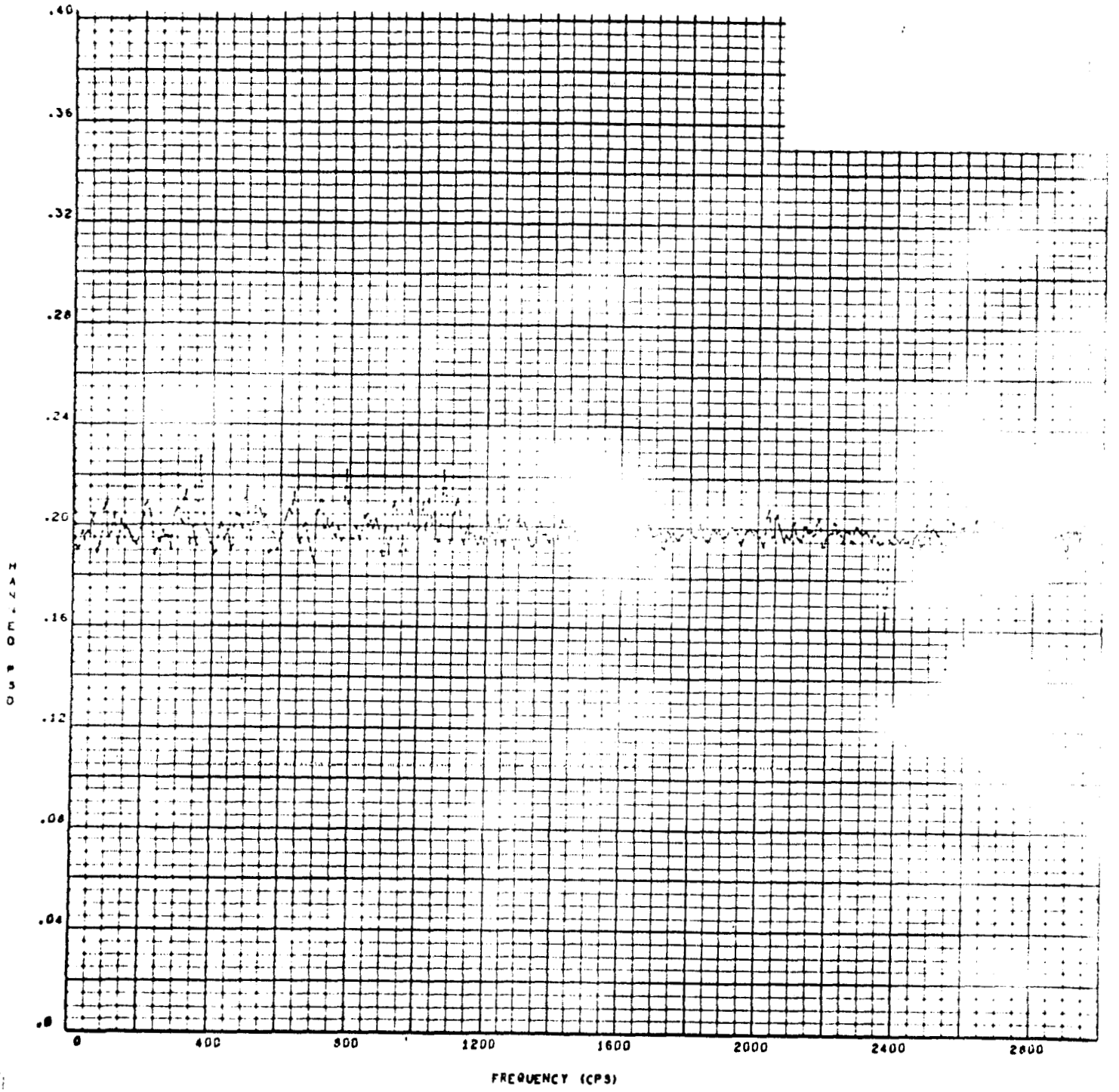
.40
.36
.32
.28
.24
.20
.16
.12
.08
.04
.0
MEAN PSD
0
400
800
1200
1600
2000
2400
2800
FREQUENCY (CPS)

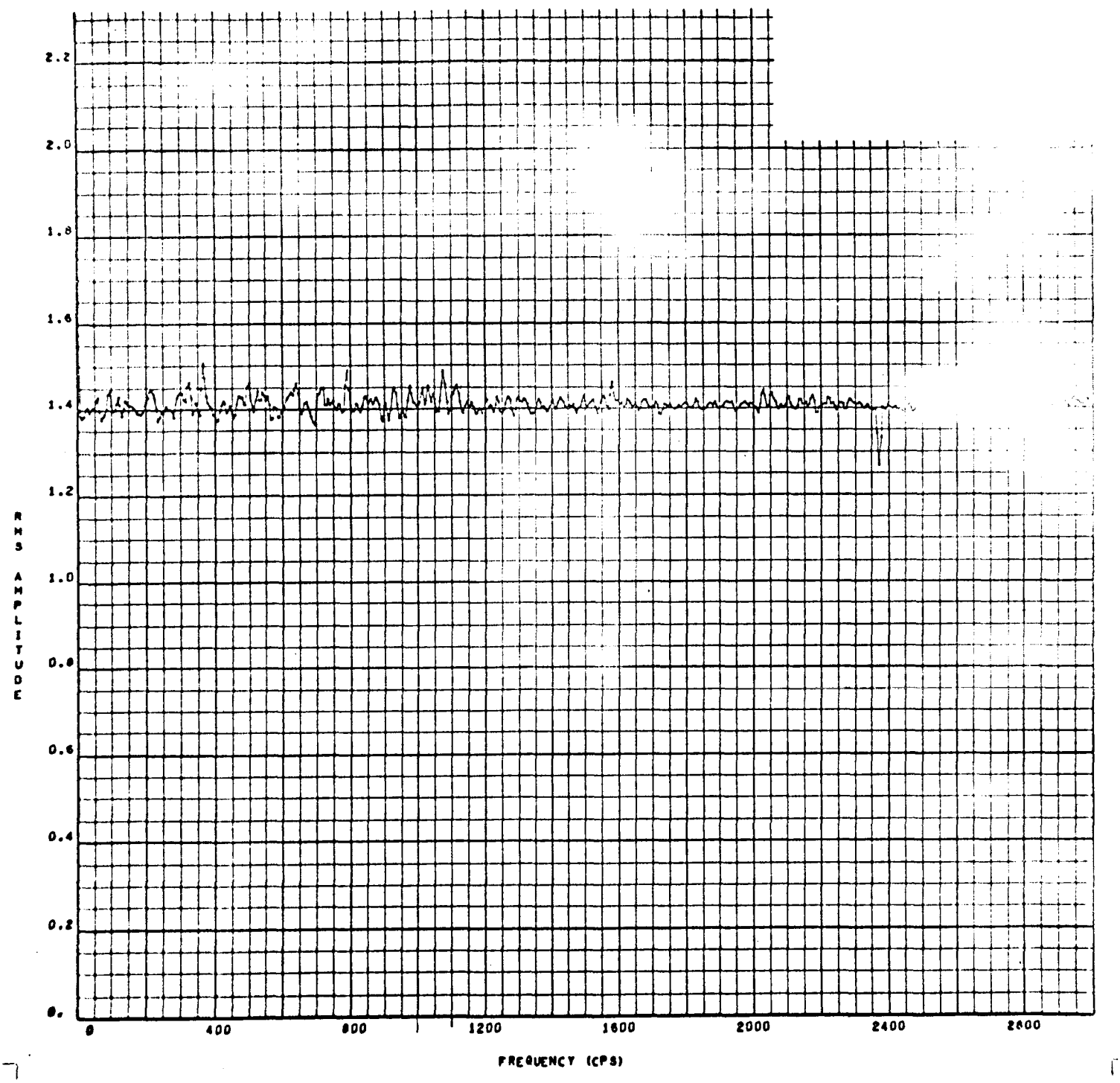
2.2
2.0
1.8
1.6
1.4
1.2
1.0
0.8
0.6
0.4
0.2
0.
RMS AMPLITUDE
0
400
800
1200
1600
2000
2400
2800
FREQUENCY (CPS)

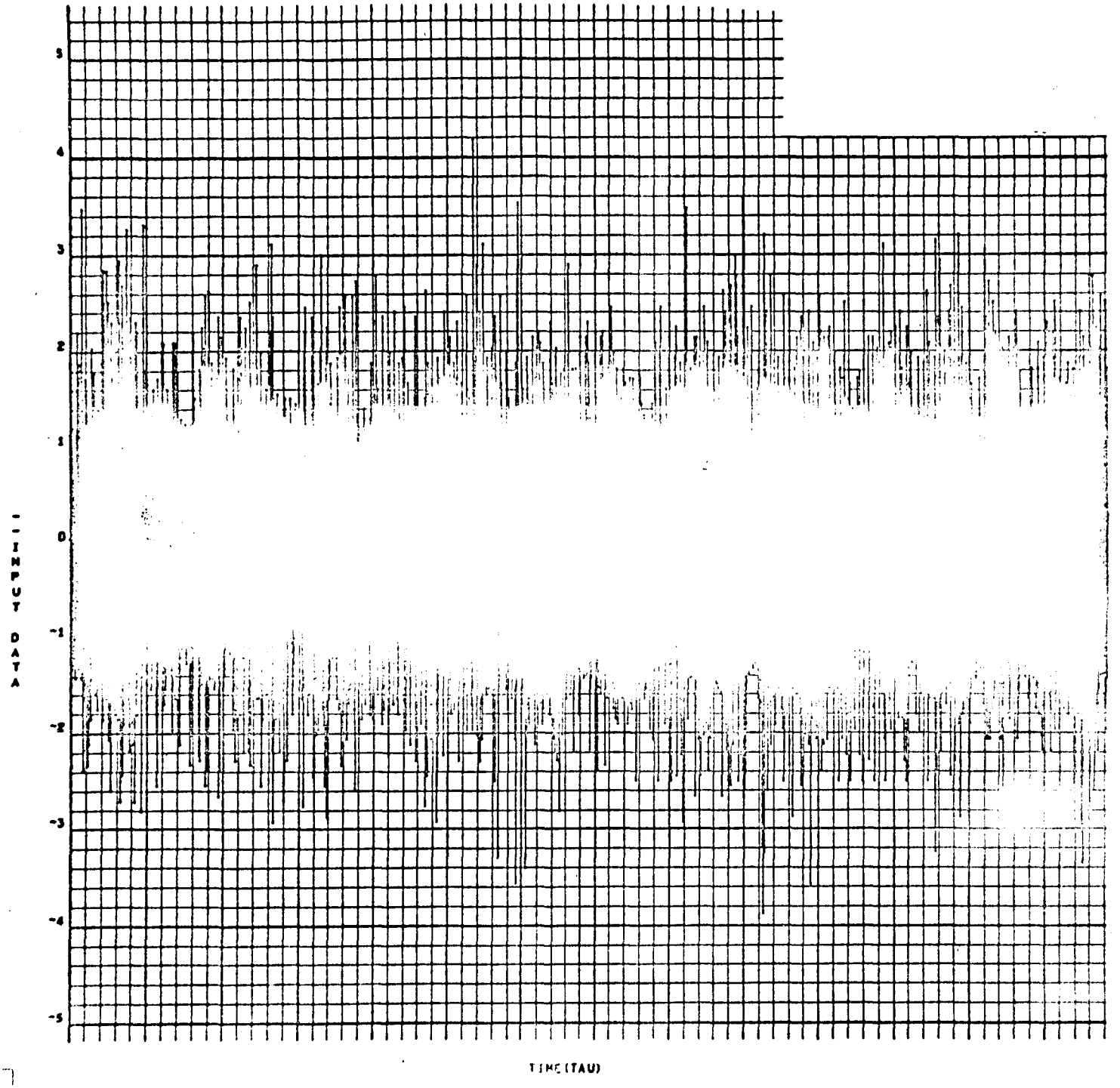

FIGURE 2.10

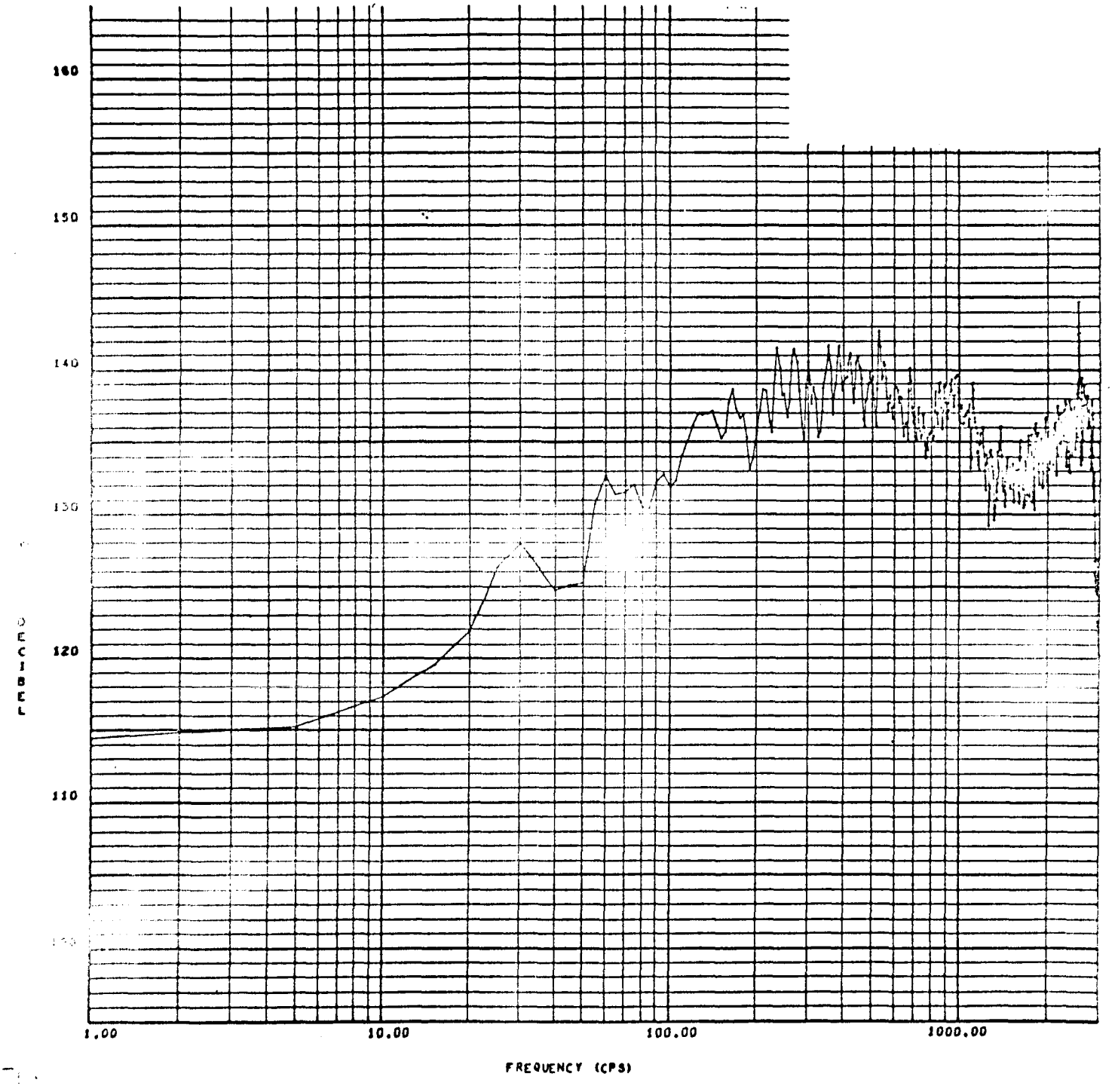

FIGURE 2.11

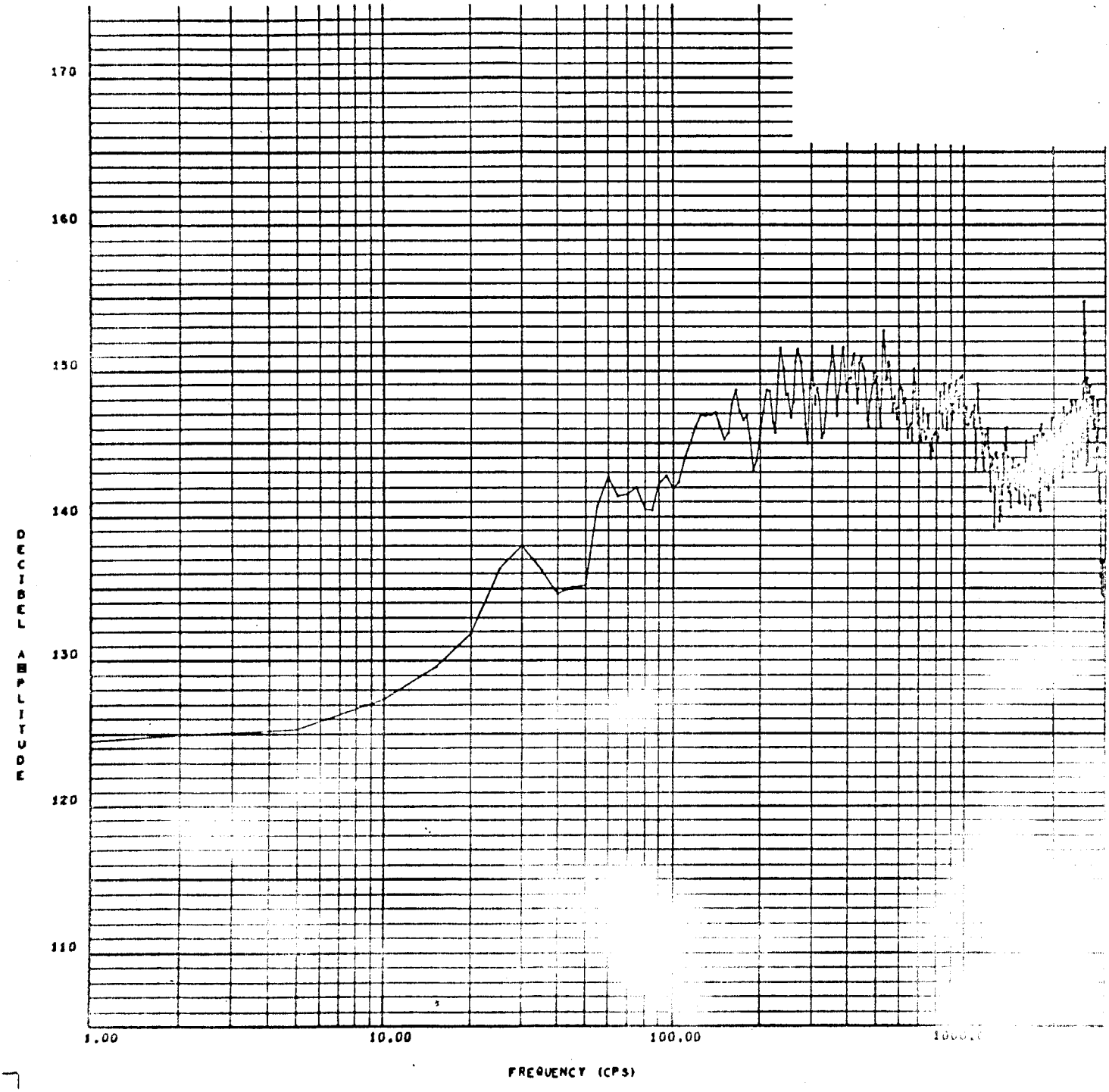
170
160
150
140
130
120
110
DECIBEL AMPLITUDE
1.00
10.00
100.00
FREQUENCY (CPS)

FIGURE 2.12

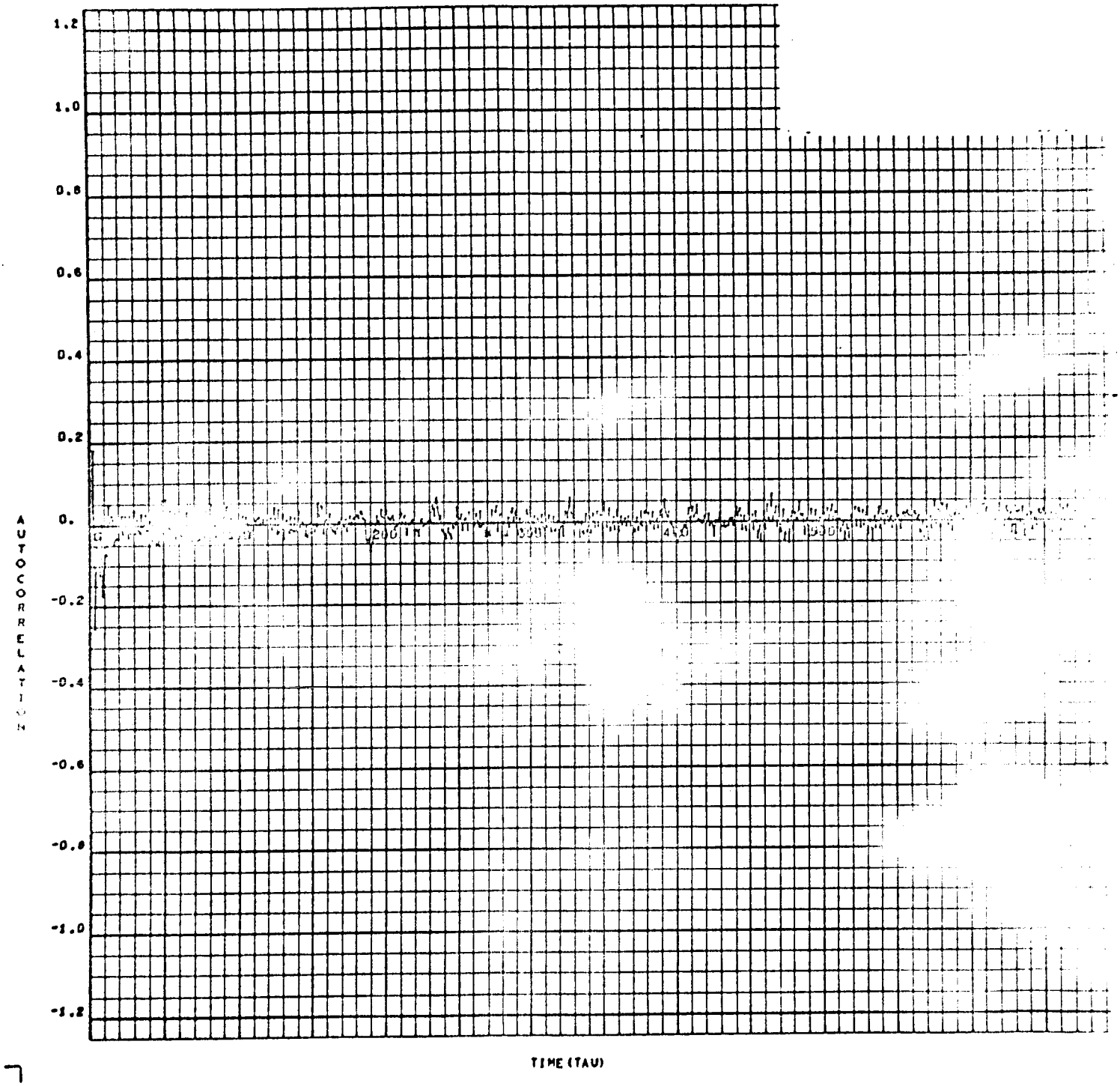

FIGURE 2.13

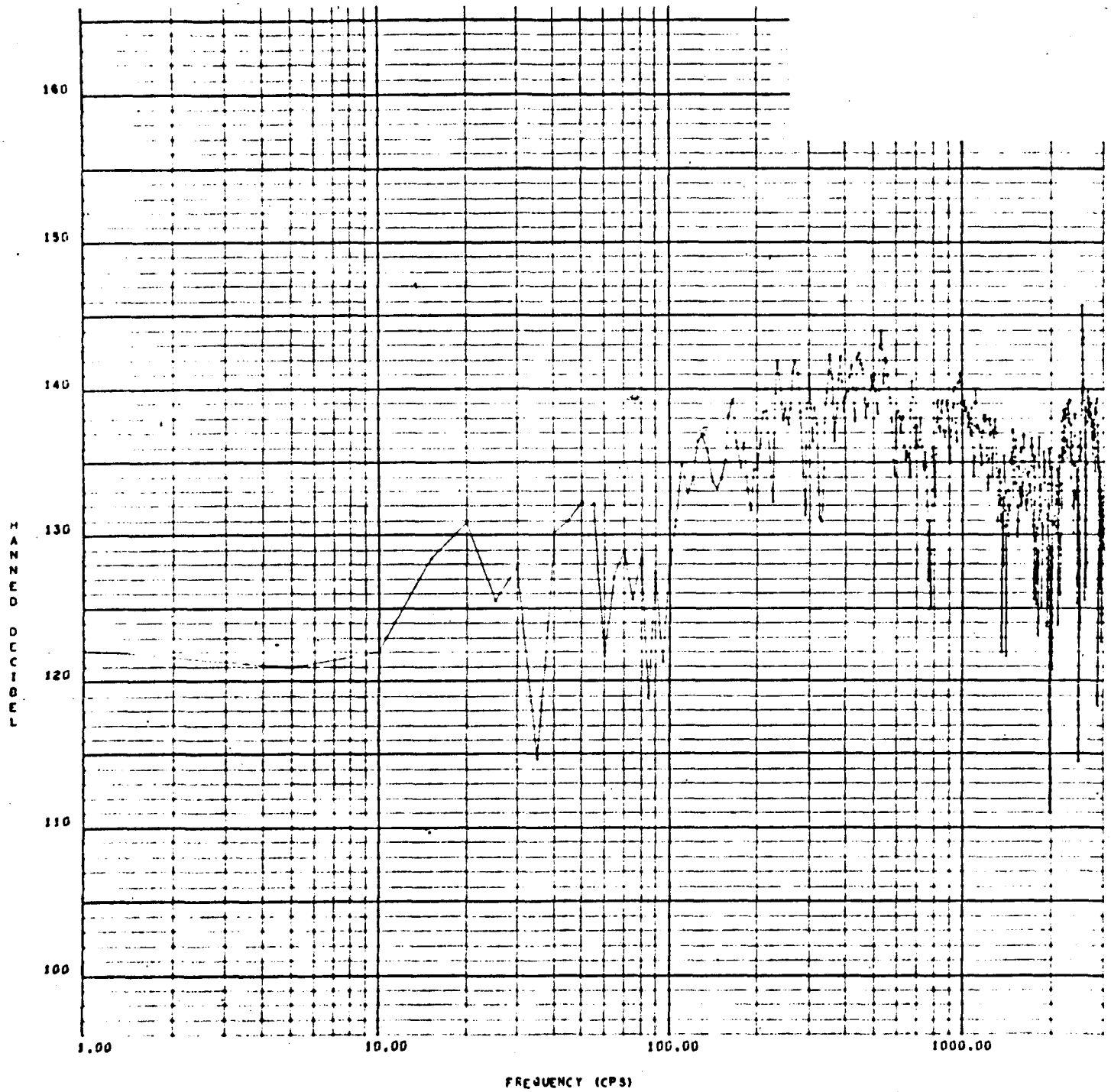
160
150
140
130
120
110
100
MANNED DECIBEL
1.00
10.00
100.00
1000.00
FREQUENCY (CPS)

FIGURE 2.21

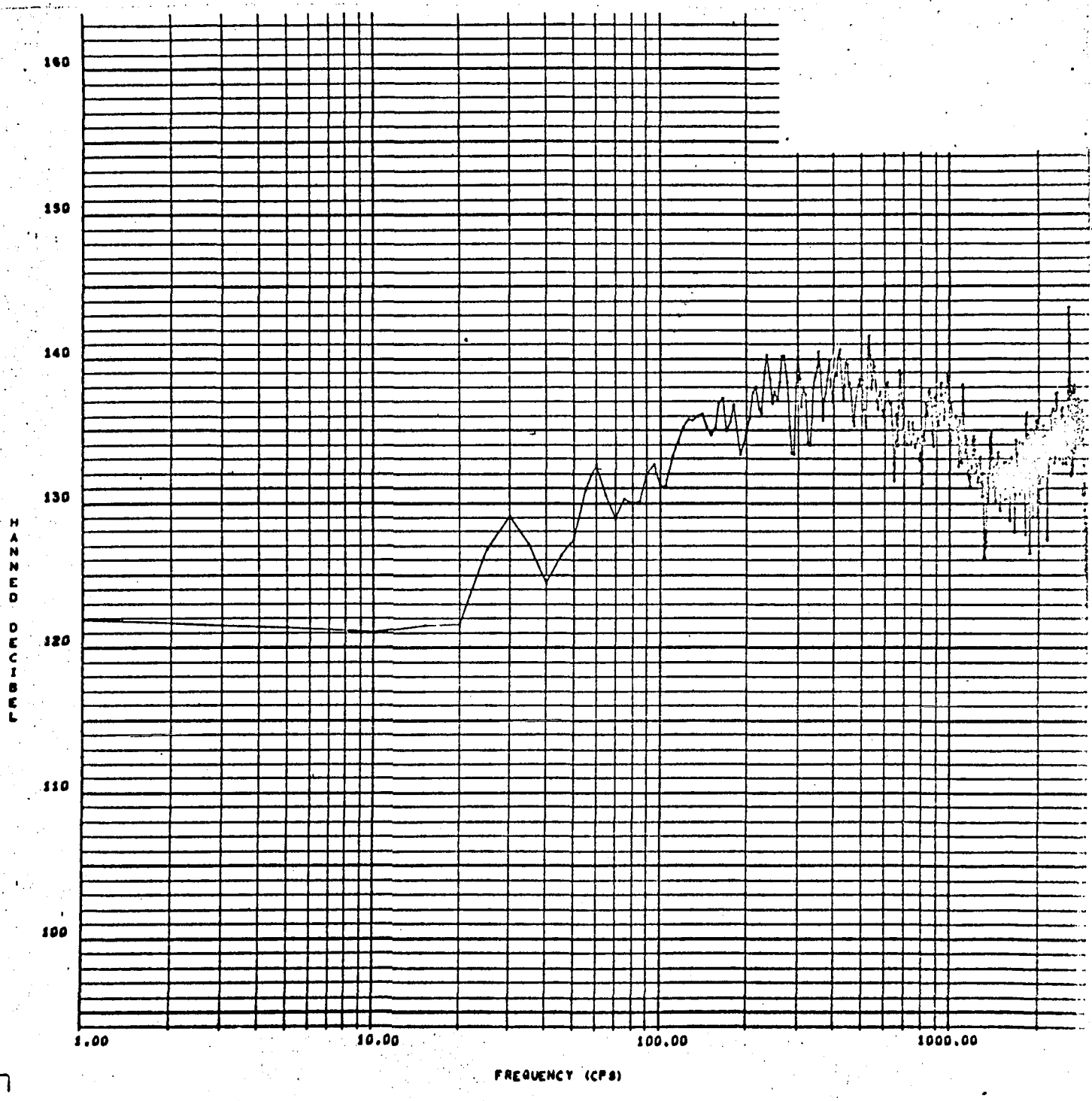
160
150
140
130
120
110
100
HANNED DECIBEL
1.00
10.00
100.00
1000.00
FREQUENCY (CPS)

FIGURE 2.31

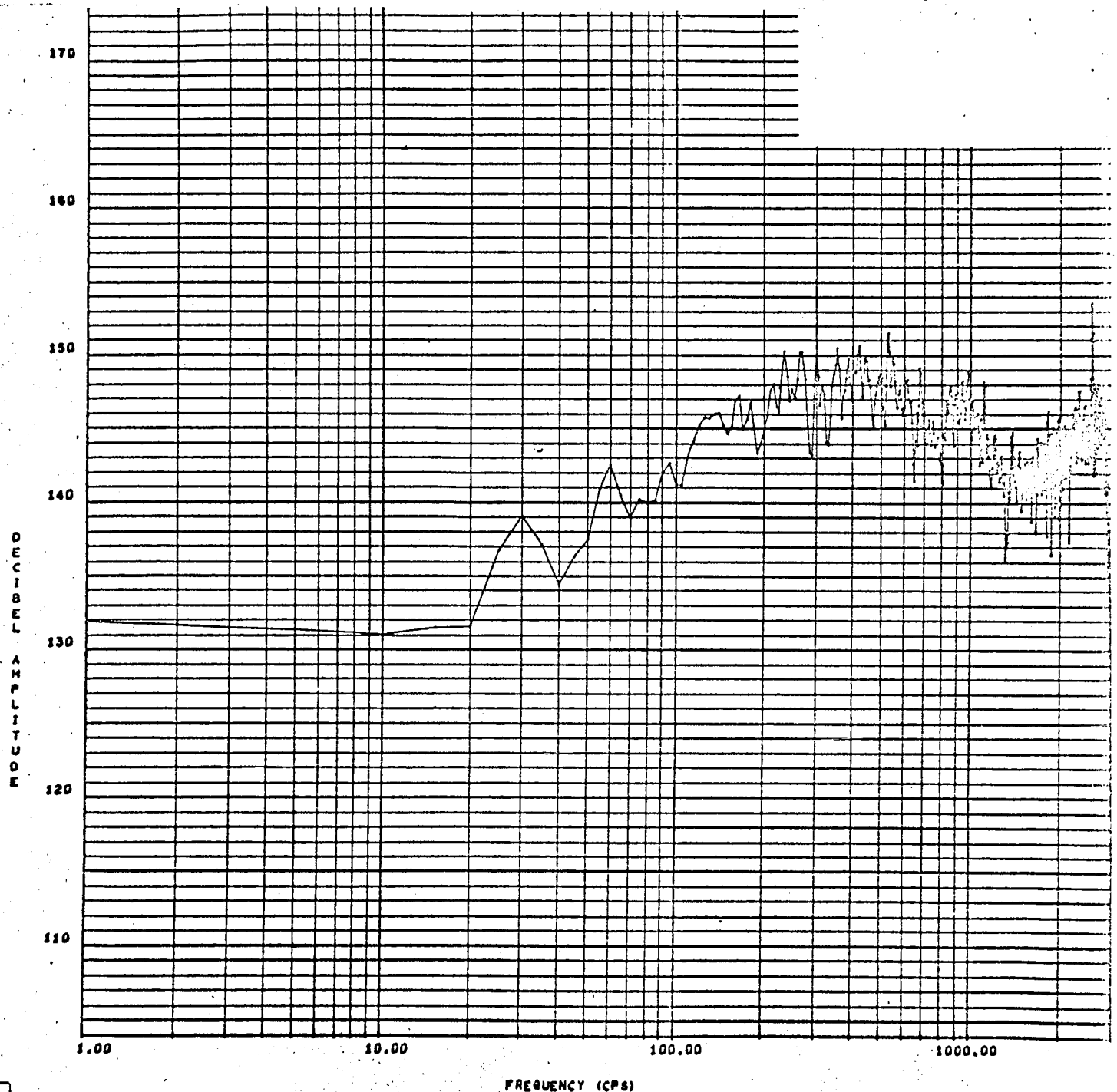
170
160
150
140
130
120
110
DECIBEL AMPLITUDE
1.00
10.00
100.00
1000.00
FREQUENCY (CPS)

FIGURE 2.32

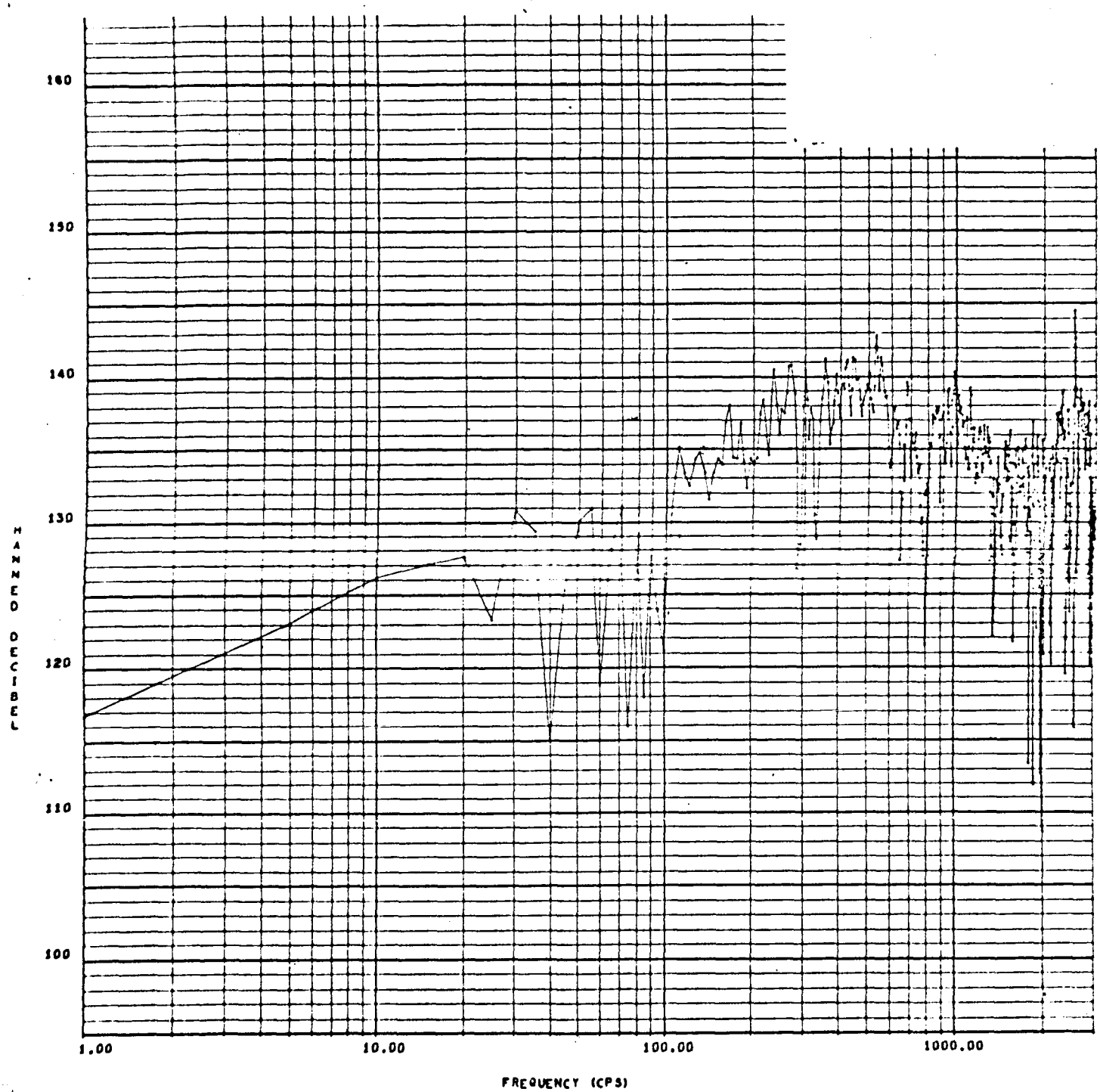
160
150
140
130
120
110
100
MANNED DECIBEL
1.00
10.00
100.00
1000.00
FREQUENCY (CPS)

FIGURE 2.41

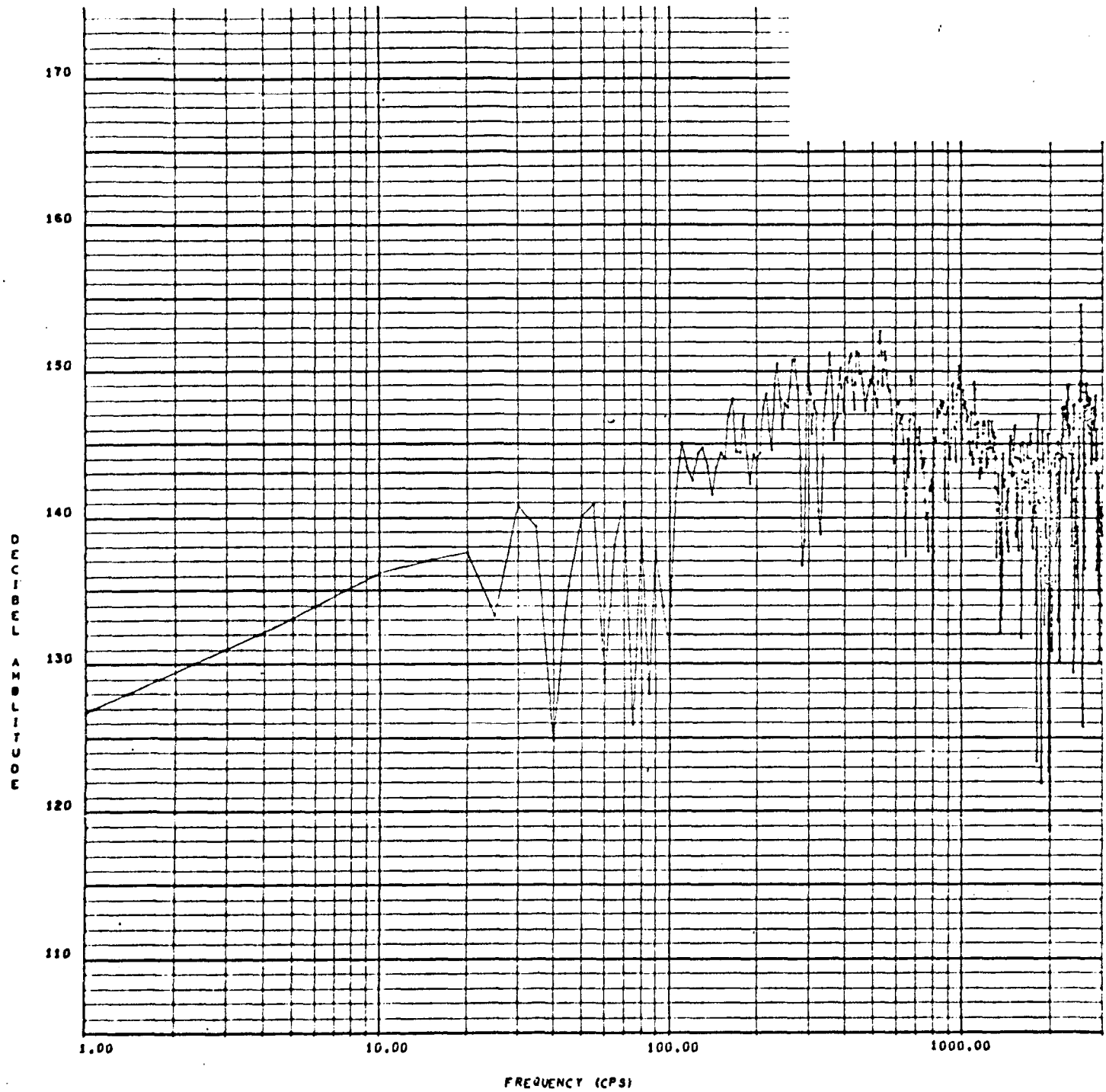
170
160
150
140
130
120
110
DECIBEL AMPLITUDE
1.00
10.00
100.00
1000.00
FREQUENCY (CPS)

FIGURE 2.42

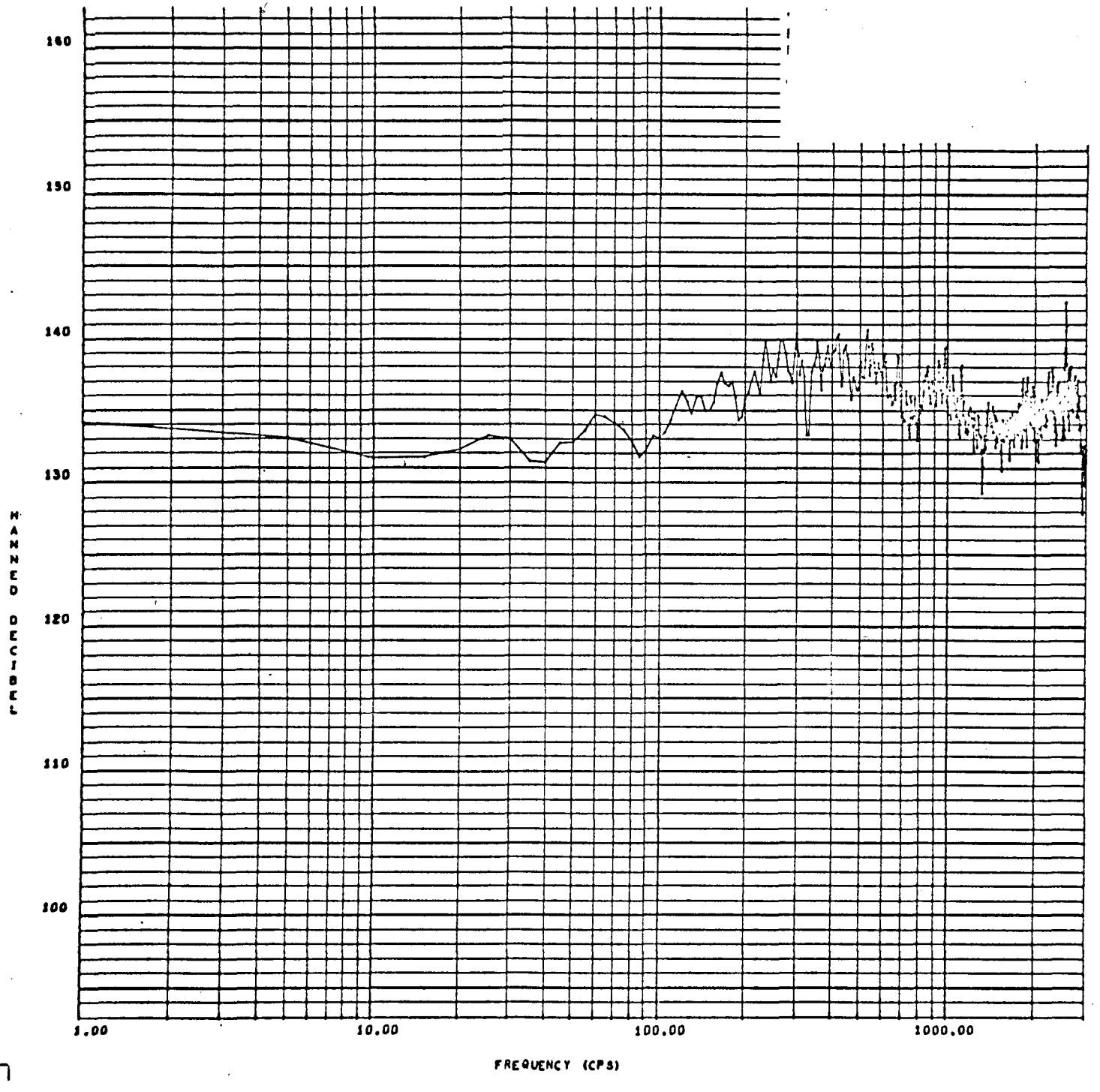
160
150
140
130
120
110
100
MANNED DECIBEL
1.00
10.00
100.00
1000.00
FREQUENCY (CPS)

FIGURE 2.51

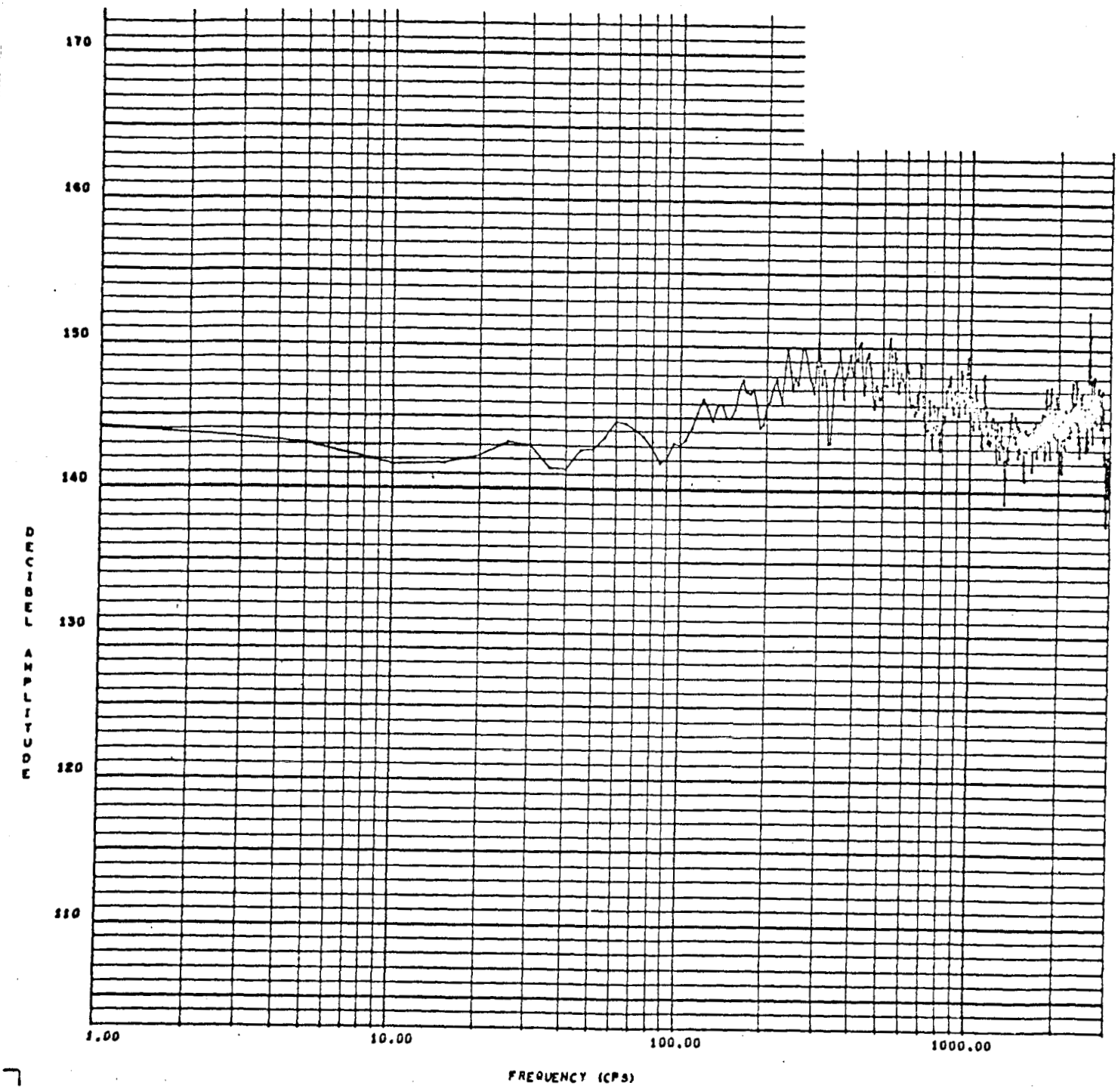
170
160
150
140
130
120
110
DECIBEL AMPLITUDE
1.00
10.00
100.00
1000.00
FREQUENCY (CPS)

FIGURE 2.52

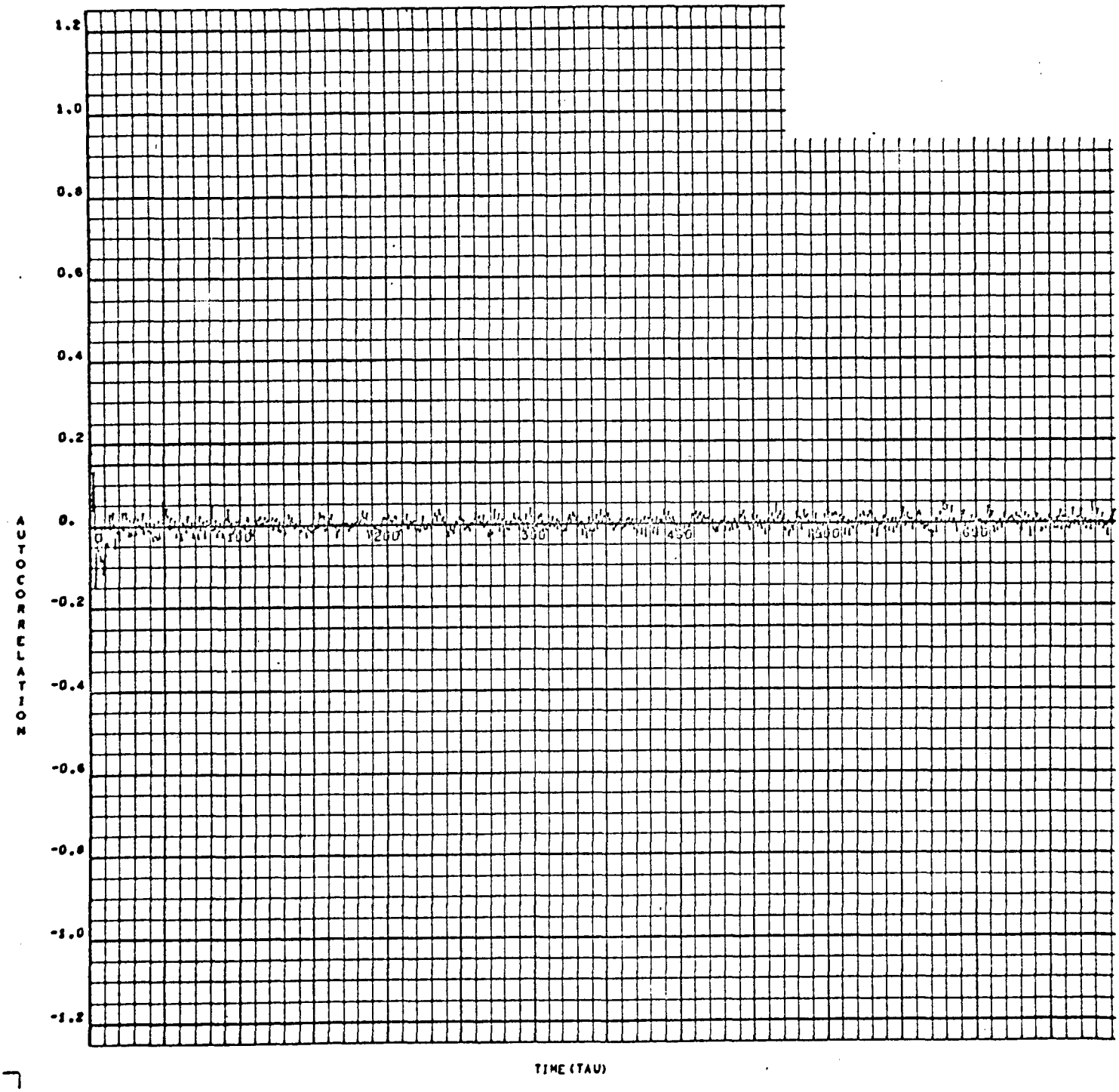
1.2
1.0
0.8
0.6
0.4
0.2
0.
-0.2
-0.4
-0.6
-0.8
-1.0
-1.2
AUTOCORRELATION
0
150
200
300
450
600
TIME (TAU)

FIGURE 2.58

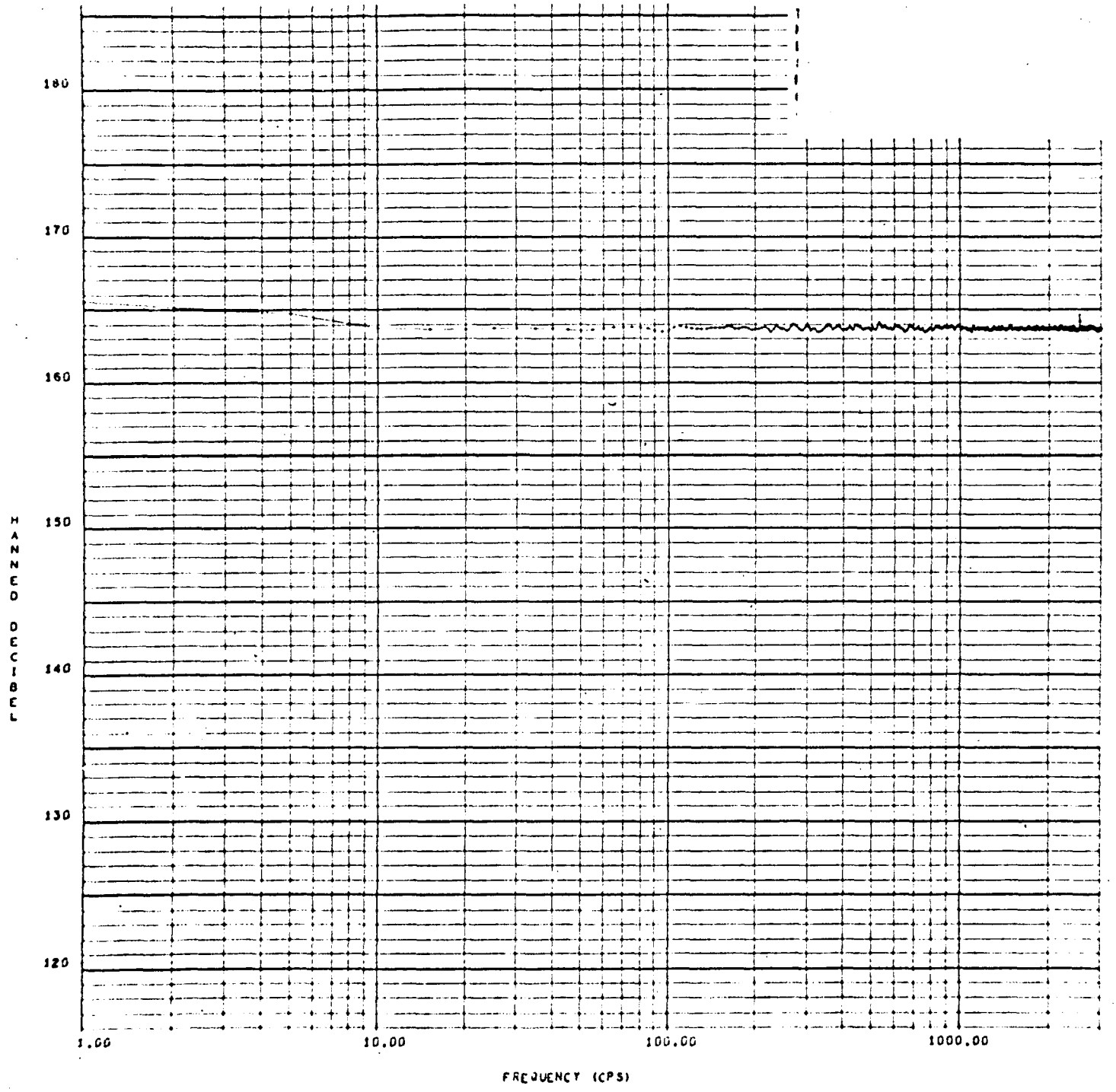
180
170
160
150
140
130
120
MANNED DECIBEL
1.00
10.00
100.00
1000.00
FREQUENCY (CPS)

FIGURE 2.61

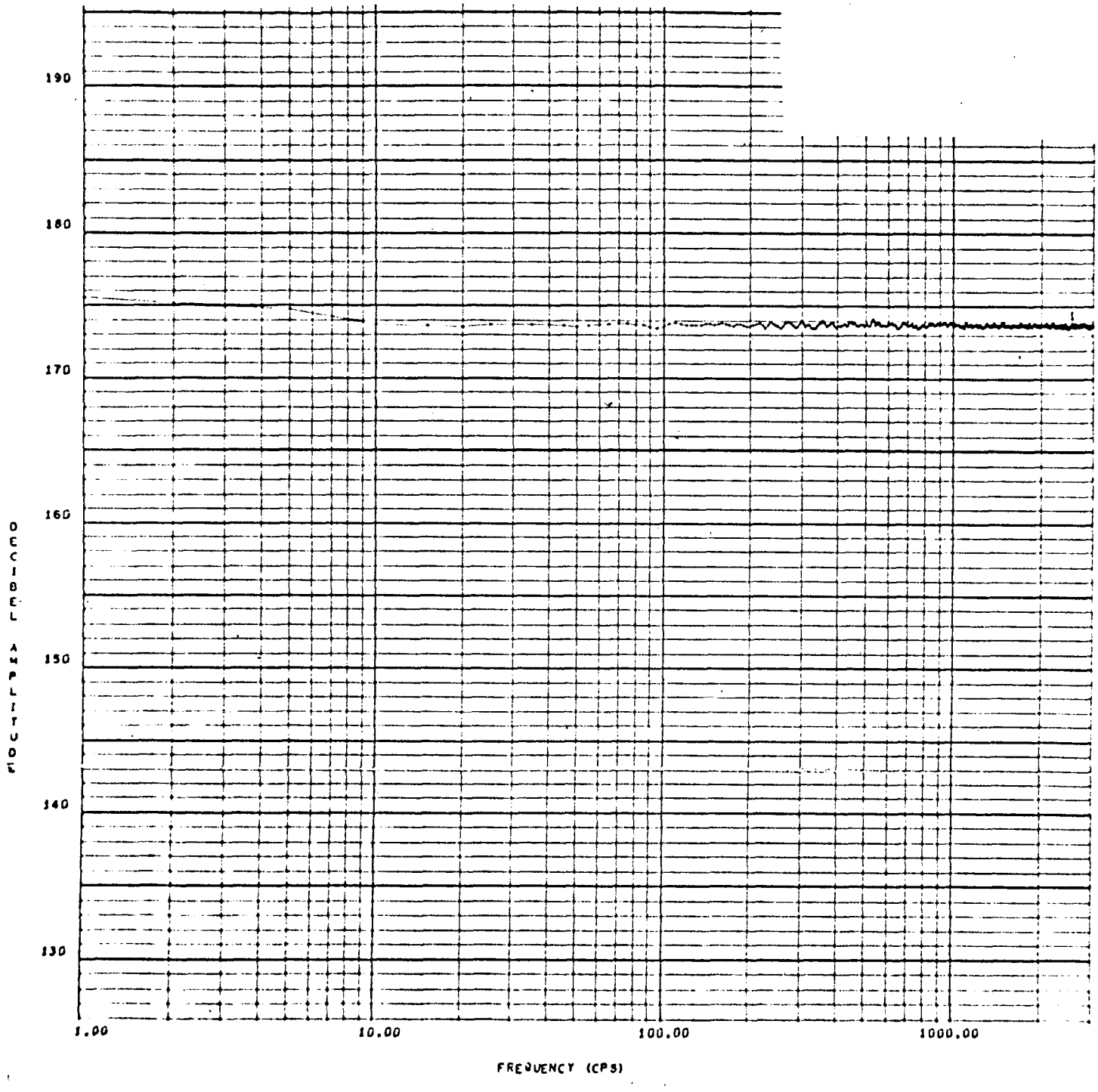
190
180
170
160
150
140
130
DECIBEL AMPLITUDE
1.00
10.00
100.00
1000.00
FREQUENCY (CPS)

FIGURE 2.62

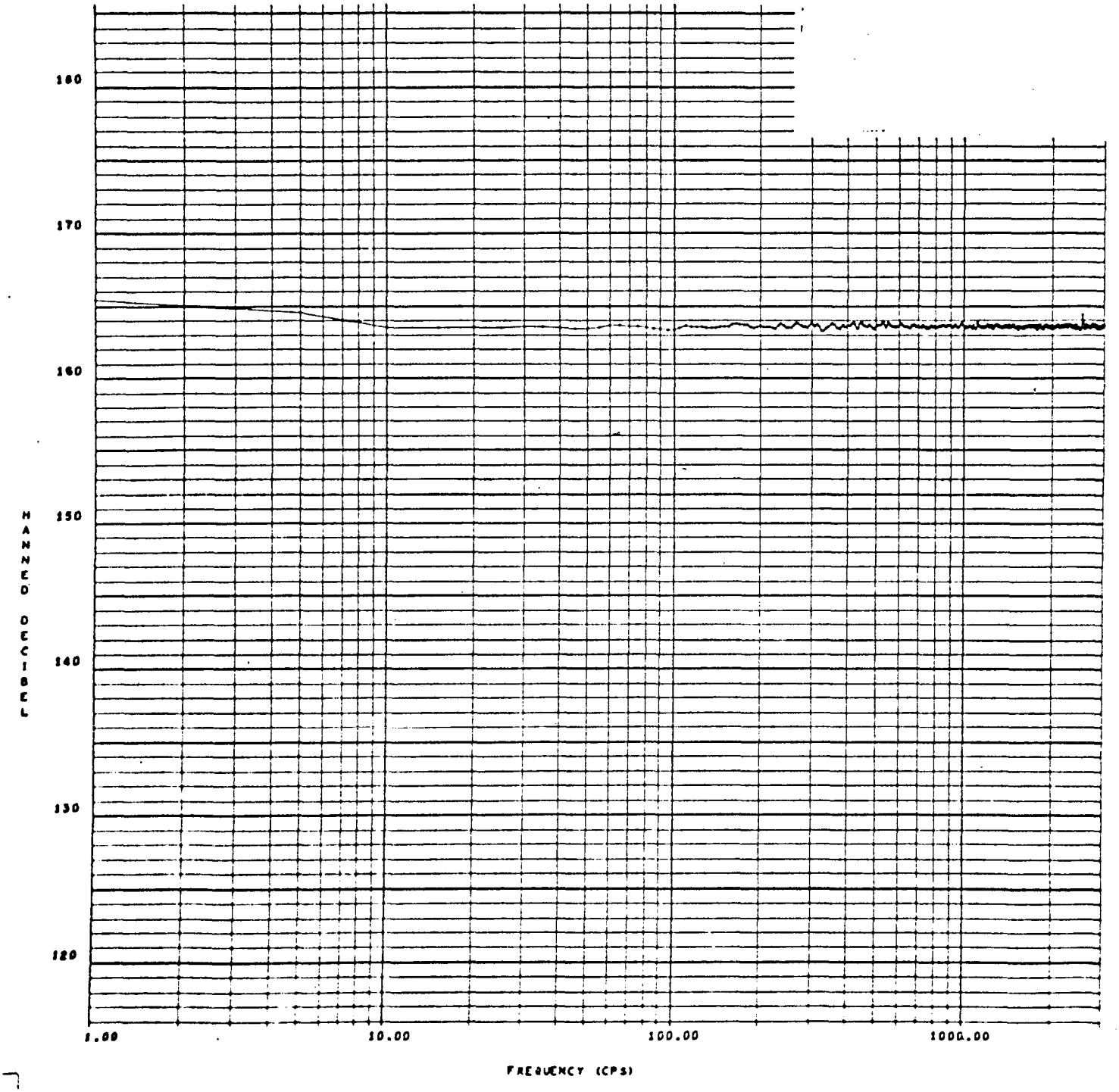
180
170
160
150
140
130
120
HANNED DECIBEL
1.00
10.00
100.00
1000.00
FREQUENCY (CPS)

FIGURE 2.71

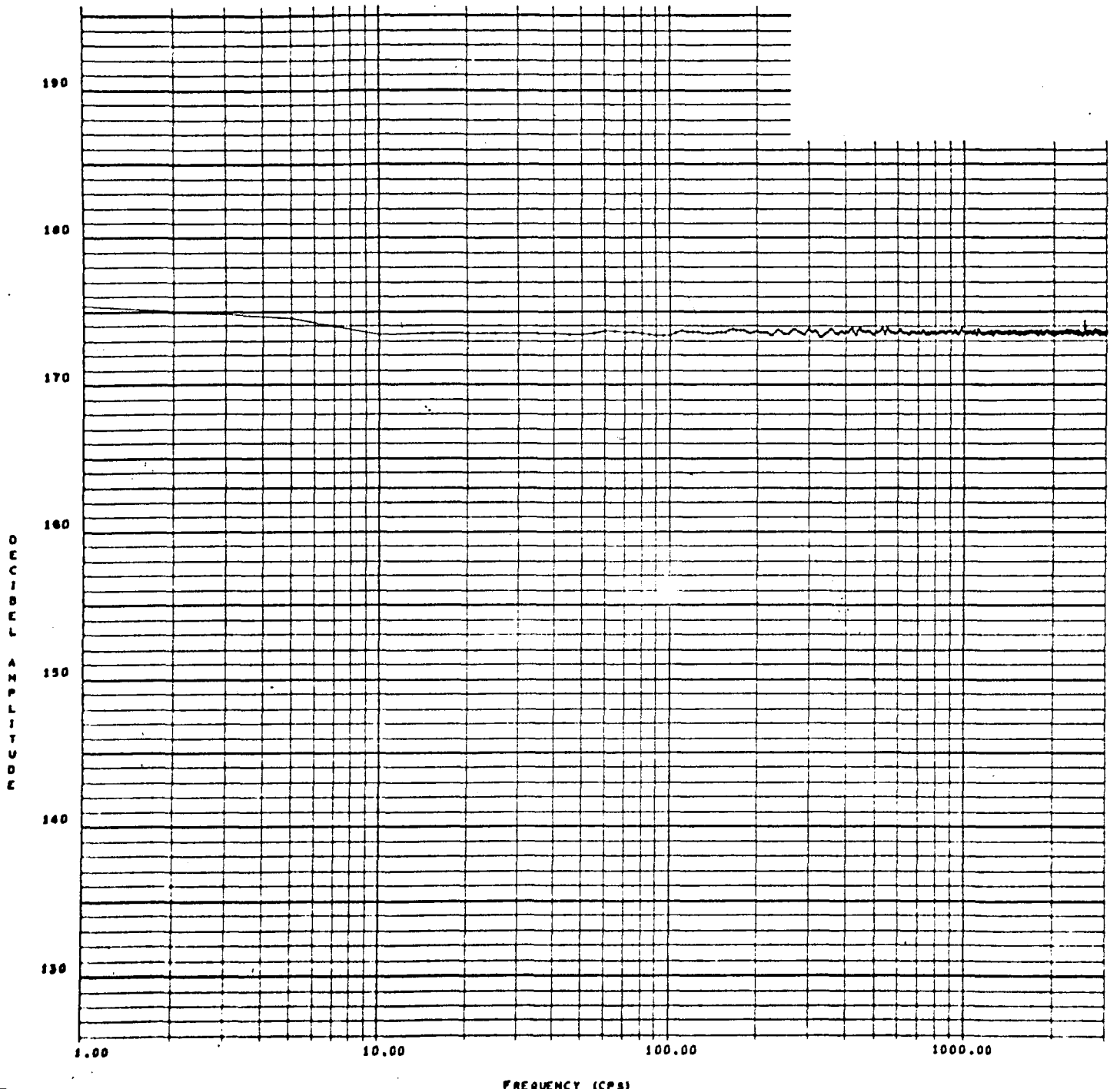
190
180
170
160
150
140
130
DECIBEL AMPLITUDE
1.00
10.00
100.00
1000.00
FREQUENCY (CPS)

FIGURE 2.72